Centrum voor Wiskunde en Informatica

REPORT RAPPORT

Multiresolution Signal Decomposition Schemes. Part 1: Linear and Morphological Pyramids

J. Goutsias and H.J.A.M. Heijmans

Probability, Networks and Algorithms (PNA)

PNA-R9810 October 1998

Report PNA-R9810
ISSN 1386-3711

CWI
P.O. Box 94079
1090 GB Amsterdam
The Netherlands

Multiresolution Signal Decomposition Schemes.

Part 1: Linear and Morphological Pyramids

John Goutsias

Center for Imaging Science
and Department of Electrical and Computer Engineering
The Johns Hopkins University, Baltimore, MD 21218, USA

Henk J.A.M. Heijmans

CWI
P.O. Box 94079, 1090 GB Amsterdam, The Netherlands

Interest in multiresolution techniques for signal processing and analysis is increasing steadily. An important instance of such a technique is the so-called pyramid decomposition scheme. This report proposes a general axiomatic pyramid decomposition scheme for signal analysis and synthesis. This scheme comprises the following ingredients: (i) the pyramid consists of a (finite or infinite) number of levels such that the information content decreases towards higher levels; (ii) each step towards a higher level is constituted by an (information-reducing) analysis operator, whereas each step towards a lower level is modeled by an (information-preserving) synthesis operator. One basic assumption is necessary: synthesis followed by analysis yields the identity operator, meaning that no information is lost by these two consecutive steps.

In this report, several examples are described of linear as well as nonlinear (e.g., morphological) pyramid decomposition schemes. Some of these examples are known from the literature (Laplacian pyramid, morphological granulometries, skeleton decomposition) and some of them are new (morphological Haar pyramid, median pyramid). Furthermore, the report makes a distinction between single-scale and multiscale decomposition schemes (i.e. without or with sample reduction).

1991 Mathematics Subject Classification: 68U10

Keywords and Phrases: Adjunction, Dilation, Erosion, Granulometry, Laplacian pyramid, Mathematical morphology, Median pyramid, Multiresolution signal processing and analysis, Multiscale morphological operators, Pyramid decomposition, Quantization, Sampling, Signal analysis and synthesis, Skeleton.

Note: Work by the second author carried out under project PNA4.3 "Morphological Image Processing." This work was supported in part by NATO Collaborative Research Grant CRG.971503. John Goutsias was also supported by the Office of Naval Research (U.S.A.), Mathematical, Computer, and Information Sciences Division, under ONR Grant N00014-90-1345.

1. Introduction

From the very early days of signal and image processing, it has been recognized that multiresolution methods are important for various reasons: (*i*) there is strong evidence that the human visual system processes information in a "multiresolution" fashion; (*ii*) signals usually consist of features of physically significant structure at different resolutions; (*iii*) sensors may provide signals of the same source at multiple resolutions; (*iv*) multiresolution algorithms offer computational advantages and, moreover, appear to be robust.

In this report, we propose a general pyramid scheme for signal analysis and synthesis. The operators involved in this scheme can be linear or nonlinear (morphological). Such a scheme encompasses various existing multiresolution approaches, such as linear (e.g. Laplacian) pyramids [1], morphological pyramids [31, 32, 12, 13, 2, 21, 23, 24, 25], median pyramids [29], morphological skeletons [27, 18, 15], and granulometries [4, 20, 27, 22, 7].

In the earliest multiresolution approaches to signal and image processing, the most popular way was to obtain a coarse level signal by subsampling a fine resolution signal, after *linear* smoothing, in order to remove high frequencies (e.g., see [33]). A *detail pyramid* can then be derived by subtracting from each level an interpolated version of the next coarser level; the best-known example is the Laplacian pyramid [1]. From a frequency point of view, the resulting difference signals (known as detail signals) form a signal decomposition in term of bandpass-filtered copies of the original signal. Moreover, there is neurophysiological evidence that the human visual system indeed uses a similar kind of decomposition [17]. This tool has been one of the most popular multiresolution schemes used in image processing and computer vision.

The previously mentioned scheme leaves a lot to be desired however, due to aliasing and use of non-ideal filters. In addition, a linear filtering approach may not be theoretically justified; in particular, the operators used for generating the various levels in a multiresolution pyramid must crucially depend on the application. The point stressed here is that coarsening an image by means of linear operators may not be compatible with a natural coarsening of some image attribute of interest (shape of object, for example), and hence use of linear procedures may be inconsistent in such applications.

In this report, we propose general multiresolution schemes which represent a signal, or image, using a sequence of successively reduced volume signals applying fixed rules that map one level to the next. In such schemes, a level is *uniquely* determined by the level below it. Our approach contains the following ingredients:

- No assumptions are made on the underlying signal/image space(s). It may be a linear space (Gaussian/Laplacian pyramid, wavelets), it may be a complete lattice (mathematical morphology), or any other set.

- The schemes are constituted by operators between different spaces (the levels of the pyramid). These operators are only required to satisfy some elementary properties and are decomposed into *analysis operators*, representing an upward step, and *synthesis operators*, representing a downward step.

Two types of multiresolution decompositions can be distinguished:

The pyramid scheme: Every analysis operator that brings a signal x_j from level j to the next coarser level $j+1$ reduces information. This information can be stored in a detail signal (at level j) which is the difference between x_j and the approximation $\hat{x}_j$ obtained by applying the synthesis operator to x_{j+1}. In general, a representation obtained by means of a pyramid (coarsest signal along with detail signals at all levels) is redundant.

The wavelet scheme: Here, the detail signal lives at level $j+1$ itself, and is obtained from a second family of analysis operators. In this case, the analysis and synthesis operators need to satisfy a condition that is very similar in nature to the biorthogonality condition known from the theory of wavelets (note, however, that this condition is formulated in operator terms only, and does not require any sort of linearity assumption or inner product). A representation obtained by means of this scheme avoids redundancy.

In this report, we exclusively deal with the pyramid scheme. The wavelet scheme will be extensively discussed in a sequel to this report. The present study shows that our pyramid decomposition scheme encompasses several existing techniques:

- *Laplacian pyramid*: This is a special case, where both the signal spaces and the operators are linear [1].
- *Morphological Skeleton*: The skeleton representation, which can be expressed in terms of morphological operations (dilation, erosion, opening, closing), is a special case of a pyramid; here the underlying signal spaces are complete lattices, and the analysis and synthesis operators are constituted by adjunctions [7].
- *Granulometries*: Granulometries and size distributions form one of the most practical concepts in mathematical morphology [27, 7]. They fit, in a most natural way, into a pyramid framework. The same appears to be true for alternating sequential filters [28, 7].
- *Morphological pyramids*: Morphological pyramids have been proposed and applied in [31, 32, 12, 13, 29, 2, 21, 23, 24, 25]. We show how such pyramids fit into our general framework, and present some new examples, as well.

This report is organized as follows. In Section 2, we recall some concepts, notations, and results of mathematical morphology that are useful throughout the report. Section 3 introduces our pyramid decomposition scheme in terms of analysis and synthesis operators and their compositions. Here, we introduce our key assumption, the *pyramid condition*, which plays a major role in our exposition. The remainder of the report is devoted to various examples and applications of our general scheme. Section 4 is concerned with linear schemes. Here, we restrict attention to schemes which are also translation invariant. Particular attention is given to the Burt-Adelson pyramid decomposition [1] and the associated Laplacian pyramid transform. Sections 5–6 are devoted to morphological pyramids. In Section 5, we consider the class of morphological pyramids based on adjunctions, and show that various morphological multiresolution techniques, such as granulometries, fit perfectly within this general framework. Moreover, an attempt to put the Lantuéjoul skeleton decomposition algorithm [27] into our framework, automatically leads to an improvement of this scheme. In Section 6, we discuss more general morphological pyramid decomposition schemes, such as median pyramids and morphological pyramids with quantization. In Section 7, we present a new class of nonlinear signal processing and analysis tools based on multiscale morphological operators. Finally, in Section 8, we end with our conclusions.

2. Mathematical Preliminaries

In this section, we provide a brief overview of some basic concepts, notations and results from the theory of mathematical morphology which we need in the sequel. A comprehensive discussion can be found in [7].

A set $\mathcal{L}$ with a partial ordering $\leq$ is called a *complete lattice* if every subset $\mathcal{K}$ of $\mathcal{L}$ has a *supremum* (least upper bound) $\bigvee \mathcal{K}$ and an *infimum* (greatest lower bound) $\bigwedge \mathcal{K}$. We say that $\mathcal{L}$

is a *complete chain* if it is a complete lattice such that $x \le y$ or $y \le x$, for every pair $x, y \in \mathcal{L}$. A simple example of a complete chain is the set $\overline{\mathbb{R}} = \mathbb{R} \cup \{-\infty, \infty\}$ with the usual ordering. Given a complete lattice $\mathcal{T}$ and a nonempty set E, the set $\mathrm{Fun}(E, \mathcal{T}) = \mathcal{T}^E$ comprising all functions $x : E \to \mathcal{T}$, is a complete lattice under the pointwise ordering

$$x \le y \quad \text{if} \quad x(p) \le y(p), \ \forall\, p \in E.$$

In this report, $\mathrm{Fun}(E, \mathcal{T})$ represents the signals with domain E and values in $\mathcal{T}$. The least and greatest elements of $\mathcal{T}$ are denoted by $\bot, \top$ respectively:

$$\bigwedge \mathcal{T} = \bot, \quad \bigvee \mathcal{T} = \top.$$

Here, we are mainly interested in the case when E is the d-dimensional discrete space $\mathbb{Z}^d$. Given a signal $x \in \mathrm{Fun}(\mathbb{Z}^d, \mathcal{T})$ and a vector $k = (k_1, k_2, \ldots, k_d) \in \mathbb{Z}^d$, we define the *translation operator* $\tau = \tau_{(k_1, k_2, \ldots, k_d)}$ by

$$(\tau x)(n) = (\tau x)(n_1, n_2, ..., n_d) = x(n_1 - k_1, n_2 - k_2, ..., n_d - k_d) = x(n - k), \quad n, k \in \mathbb{Z}^d.$$

Given a mapping $\psi : \mathrm{Fun}(\mathbb{Z}^d, \mathcal{T}) \to \mathrm{Fun}(\mathbb{Z}^d, \mathcal{T})$, we say that ψ is *translation invariant* if

$$\psi \tau = \tau \psi, \tag{2.1}$$

for every translation operator τ.

Two basic morphological operators on $\mathrm{Fun}(\mathbb{Z}^d, \mathcal{T})$ are the (flat) *dilation* δ_A and the (flat) *erosion* ε_A, given by:

$$\delta_A(x)(n) = (x \oplus A)(n) = \bigvee_{k \in A} x(n - k) \tag{2.2}$$

$$\varepsilon_A(x)(n) = (x \ominus A)(n) = \bigwedge_{k \in A} x(n + k). \tag{2.3}$$

Here, $A \subseteq \mathbb{Z}^d$ is a given set, the so-called *structuring element*. There exists an important relation for dilations and erosions:

$$y \oplus A \le x \iff y \le x \ominus A, \quad x, y \in \mathrm{Fun}(\mathbb{Z}^d, \mathcal{T}).$$

This relation, called the *adjunction relation*, forms the key ingredient for the so-called *complete lattice framework* of mathematical morphology. We briefly discuss this framework below, since it plays an important role throughout this report.

2.1. Definition. Consider two complete lattices $\mathcal{L}$ and $\mathcal{M}$, and two operators $\varepsilon : \mathcal{L} \to \mathcal{M}$ and $\delta : \mathcal{M} \to \mathcal{L}$. We say that (ε, δ) constitutes an adjunction between $\mathcal{L}$ and $\mathcal{M}$ if

$$\delta(y) \le x \iff y \le \varepsilon(x), \quad x \in \mathcal{L}, \ y \in \mathcal{M}.$$

If (ε, δ) forms an adjunction between $\mathcal{L}$ and $\mathcal{M}$, then ε has the property

$$\varepsilon(\bigwedge_{i \in I} x_i) = \bigwedge_{i \in I} \varepsilon(x_i), \tag{2.4}$$

for any family of signals $\{x_i \mid i \in I\} \subseteq \mathcal{L}$. Operator δ has the dual property

$$\delta(\bigvee_{i \in I} y_i) = \bigvee_{i \in I} \delta(y_i), \tag{2.5}$$

for any family of signals $\{y_i \mid i \in I\} \subseteq \mathcal{M}$. This implies in particular that ε and δ are increasing (i.e., monotone) operators. An operator ε that satisfies (2.4) is called an *erosion*, whereas an operator δ that satisfies (2.5) is called a *dilation*. We denote the identity operator on $\mathcal{L}$ by $\mathsf{id}_{\mathcal{L}}$, or simply id, when there is no danger of confusion. The following propositions hold.

2.2. Proposition.

(a) *With every erosion* $\varepsilon : \mathcal{L} \to \mathcal{M}$*, there corresponds a unique dilation* $\delta : \mathcal{M} \to \mathcal{L}$ *such that* (ε, δ) *constitutes an adjunction.*

(b) *With every dilation* $\delta : \mathcal{M} \to \mathcal{L}$*, there corresponds a unique erosion* $\varepsilon : \mathcal{L} \to \mathcal{M}$ *such that* (ε, δ) *constitutes an adjunction.*

2.3. Proposition. *Let* (ε, δ) *be an adjunction between two complete lattices* $\mathcal{L}$ *and* $\mathcal{M}$*. The following holds:*

$$\varepsilon\delta\varepsilon = \varepsilon \quad \text{and} \quad \delta\varepsilon\delta = \delta$$
$$\varepsilon\delta \geq \mathsf{id} \quad \text{and} \quad \delta\varepsilon \leq \mathsf{id}.$$

An operator ν on a complete lattice $\mathcal{L}$ is a *negation*, if it is a bijection that reverses ordering (i.e., $x \leq y \Rightarrow \nu(y) \leq \nu(x)$) such that $\nu^2 = \mathsf{id}$, the identity operator. For example, for every $x \in \text{Fun}(E, \mathcal{T})$, $\nu(x) = -x$, if $\mathcal{T} = \overline{\mathbb{R}}$, whereas $\nu(x) = N - 1 - x$, if $\mathcal{T} = \{0, 1, ..., N-1\}$. Let $\mathcal{L}$, $\mathcal{M}$ be two complete lattices with negations $\nu_{\mathcal{L}}$, $\nu_{\mathcal{M}}$, respectively. With an operator ψ: $\mathcal{L} \to \mathcal{M}$, we can associate the *negative operator* $\psi^* = \nu_{\mathcal{M}}\psi\nu_{\mathcal{L}}$. When no confusion about the respective negation seems possible, we set $\psi^*(x) = [\psi(x^*)]^*$. If (ε, δ) forms an adjunction between two complete lattices $\mathcal{L}$ and $\mathcal{M}$, and if both lattices have a negation, then the pair $(\delta^*, \varepsilon^*)$ forms an adjunction between $\mathcal{M}$ and $\mathcal{L}$ as well.

We now need the following definition.

2.4. Definition. Let ψ be an operator from a complete lattice $\mathcal{L}$ into itself.

(a) ψ is *idempotent*, if $\psi^2 = \psi$.

(b) If ψ is increasing and idempotent, then ψ is a (*morphological*) *filter.*

(c) A filter ψ which satisfies $\psi \leq \mathsf{id}$ (ψ is anti-extensive) is an *opening.*

(d) A filter ψ which satisfies $\psi \geq \mathsf{id}$ (ψ is extensive) is a *closing.*

2.5. Proposition. *Let* (ε, δ) *be an adjunction between two complete lattices* $\mathcal{L}$ *and* $\mathcal{M}$*. Then,* $\varepsilon\delta$ *is a closing on* $\mathcal{M}$ *and* $\delta\varepsilon$ *is an opening on* $\mathcal{L}$*.*

We have seen that the pair $(\varepsilon_A, \delta_A)$, given by (2.2) and (2.3), constitutes an adjunction on $\text{Fun}(\mathbb{Z}^d, \mathcal{T})$. Thus, we may conclude that the composition $\alpha_A = \delta_A\varepsilon_A$ is an opening whereas the composition $\beta_A = \varepsilon_A\delta_A$ is a closing, in the sense of Definition 2.4. Operators α_A and β_A are called the *opening* and *closing* by A, respectively. We use the following notation:

$$\alpha_A(x) = x \bigcirc A \tag{2.6}$$
$$\beta_A(x) = x \bullet A. \tag{2.7}$$

3. Multiresolution Signal Decomposition

To obtain a mathematical representation for a multiresolution signal decomposition scheme, we need a sequence of signal domains, assigned at each level of the scheme, and analysis/synthesis operators that map information between different levels. The analysis operators are designed to reduce information in order to simplify signal representation whereas the synthesis operators are designed to undo as much as possible this loss of information. This is a widely accepted approach to multiresolution signal decomposition [3, 33, 16]. Moreover, as discussed in the introduction, the analysis/synthesis operators depend on the application at hand and a sound theory should be able to treat them from a general point of view. Motivated by these reasons, we propose in this section a general multiresolution signal decomposition scheme, to be referred to as the *pyramid transform.*

3.1. Analysis and synthesis operators

Let $J \subseteq \mathbb{Z}$ be an index set indicating the levels in a multiresolution signal decomposition scheme. We either consider J to be finite or infinite. In the finite case, we take $J = \{0, 1, \ldots, K\}$, for some $K < \infty$, whereas $J = \{0, 1, \ldots\}$ in the infinite case. A domain V_j of signals is assigned at each level j. No particular assumptions on V_j are made at this point (e.g., it is not necessarily true that V_j is a linear space). In this framework, *signal analysis* consists of decomposing a signal in the direction of increasing j. This task is accomplished by means of *analysis operators* $\psi_j^\uparrow : V_j \to V_{j+1}$. On the other hand, *signal synthesis* proceeds in the direction of decreasing j, by means of *synthesis operators* $\psi_j^\downarrow : V_{j+1} \to V_j$. Here, the upward arrow indicates that the operator $\psi^\uparrow$ maps a signal to a level higher in the pyramid, whereas the downward arrow indicates that the operator $\psi^\downarrow$ maps a signal to a level lower in the pyramid. The analysis operator $\psi_j^\uparrow$ is designed to reduce information in order to simplify signal representation at level $j+1$, whereas the synthesis operator $\psi_j^\downarrow$ is designed to map this information back to level j.

We can travel from any level i in the pyramid to a higher level j by successively composing analysis operators. This gives an operator

$$\psi_{i,j}^\uparrow = \psi_{j-1}^\uparrow \psi_{j-2}^\uparrow \cdots \psi_i^\uparrow, \quad j > i, \tag{3.1}$$

which maps an element in V_i to an element in V_j. On the other hand, the composed synthesis operator

$$\psi_{j,i}^\downarrow = \psi_i^\downarrow \psi_{i+1}^\downarrow \cdots \psi_{j-1}^\downarrow, \quad j > i, \tag{3.2}$$

takes us back from level j to level i. Finally, we define the composition

$$\hat{\psi}_{i,j} = \psi_{j,i}^\downarrow \psi_{i,j}^\uparrow, \quad j > i, \tag{3.3}$$

which takes a signal from level i to level j and back to level i again.

The analysis operators $\psi_j^\uparrow$ are designed to reduce signal information. Hence, they are not invertible in general, and information loss cannot be recovered by using only the synthesis operators $\psi_j^\downarrow$. Therefore, $\hat{\psi}_{i,j}$ can be regarded as an *approximation operator* that approximates a signal at level i, by mapping (by means of $\psi_{j,i}^\downarrow$) the reduced information at level j, incurred by $\psi_{i,j}^\uparrow$, back to level i.

We now state a number of conditions that are crucial to what follows.

3.1. Condition.

(a) $\psi_j^\uparrow$ is surjective
(b) $\psi_j^\downarrow$ is injective
(c) $\psi_j^\uparrow \psi_j^\downarrow \psi_j^\uparrow = \psi_j^\uparrow$
(d) $\psi_j^\downarrow \psi_j^\uparrow \psi_j^\downarrow = \psi_j^\downarrow$
(e) $\psi_j^\downarrow \psi_j^\uparrow$ is idempotent; i.e., $\psi_j^\downarrow \psi_j^\uparrow \psi_j^\downarrow \psi_j^\uparrow = \psi_j^\downarrow \psi_j^\uparrow$
(f) $\psi_j^\uparrow \psi_j^\downarrow = \mathsf{id}$ on V_{j+1}.

Here, id denotes the identity operator on V_{j+1}. The first condition is required in order to assure that for any signal $y \in V_{j+1}$ there always exists a signal $x \in V_j$ such that $y = \psi_j^\uparrow(x)$. This condition is easily satisfied by setting $V_{j+1} = \mathrm{Ran}(\psi_j^\uparrow)$ (i.e., the range of the analysis operator $\psi_j^\uparrow$). That $\psi_j^\uparrow$ is only surjective (and not necessarily injective) formalizes the fact that $\psi_j^\uparrow$ gives rise to a loss of signal information (i.e., there might be two signals $x_1, x_2 \in V_j$, $x_1 \neq x_2$, such that $\psi_j^\uparrow(x_1) = \psi_j^\uparrow(x_2)$). The second condition guarantees that application of the synthesis operator

$\psi_j^{\downarrow}$ does not result in an additional loss of signal information (i.e., if $x_1, x_2 \in V_{j+1}$ such that $x_1 \neq x_2$, then $\psi_j^{\downarrow}(x_1) \neq \psi_j^{\downarrow}(x_2)$). In principle, given signal $\psi_{j,i}^{\downarrow}(x) \in V_i$, where $x \in V_j$ and $j > i$, we should always be able to uniquely recover x. The fifth condition guarantees that the signal decomposition is non-redundant, in the sense that repeated application of the analysis/synthesis steps does not modify the decomposition.

We can establish a number of relationships between the previous conditions.

3.2. Proposition. *The following relationships between the previous conditions are true:*

$(c) \;\Rightarrow\; (e)$ *and* $(d) \;\Rightarrow\; (e)$

$(a),(b),(e) \iff (a),(c) \iff (b),(d) \iff (f)$

PROOF. $(c) \Rightarrow (e)$: Since $\psi_j^{\uparrow}\psi_j^{\downarrow}\psi_j^{\uparrow} = \psi_j^{\uparrow}$, we have that $\psi_j^{\downarrow}\psi_j^{\uparrow}\psi_j^{\downarrow}\psi_j^{\uparrow} = \psi_j^{\downarrow}\psi_j^{\uparrow}$ which shows idempotence.

$(d) \Rightarrow (e)$: Since $\psi_j^{\downarrow}\psi_j^{\uparrow}\psi_j^{\downarrow} = \psi_j^{\downarrow}$, we have that $\psi_j^{\downarrow}\psi_j^{\uparrow}\psi_j^{\downarrow}\psi_j^{\uparrow} = \psi_j^{\downarrow}\psi_j^{\uparrow}$ which shows idempotence.

$(a),(c) \Rightarrow (b)$: Take $y_1, y_2 \in V_{j+1}$ such that $y_1 \neq y_2$. Since $\psi_j^{\uparrow}$ is surjective, there always exist signals $x_1, x_2 \in V_j$ such that $y_1 = \psi_j^{\uparrow}(x_1)$ and $y_2 = \psi_j^{\uparrow}(x_2)$, from which we have that $\psi_j^{\uparrow}(x_1) \neq \psi_j^{\uparrow}(x_2)$, or $x_1 \neq x_2$. In this case, $\psi_j^{\uparrow}\psi_j^{\downarrow}(y_1) = \psi_j^{\uparrow}\psi_j^{\downarrow}\psi_j^{\uparrow}(x_1) = \psi_j^{\uparrow}(x_1) \neq \psi_j^{\uparrow}(x_2) = \psi_j^{\uparrow}\psi_j^{\downarrow}\psi_j^{\uparrow}(x_2) = \psi_j^{\uparrow}\psi_j^{\downarrow}(y_2)$, which implies that $\psi_j^{\downarrow}(y_1) \neq \psi_j^{\downarrow}(y_2)$. Therefore, $\psi_j^{\downarrow}$ is injective.

$(b),(d) \Rightarrow (a)$: Take $y \in V_{j+1}$. From (d), we have that $\psi_j^{\downarrow}\psi_j^{\uparrow}\psi_j^{\downarrow}(y) = \psi_j^{\downarrow}(y)$ which, together with the fact that $\psi_j^{\downarrow}$ is injective, implies that $\psi_j^{\uparrow}\psi_j^{\downarrow}(y) = y$, or $y = \psi_j^{\uparrow}(x)$, where $x = \psi_j^{\downarrow}(y)$. This shows that $\psi_j^{\uparrow}$ is surjective.

$(f) \;\Rightarrow\; (b),(d)$: Since $\psi_j^{\uparrow}\psi_j^{\downarrow} = \mathsf{id}$, we have that $\psi_j^{\downarrow}\psi_j^{\uparrow}\psi_j^{\downarrow} = \psi_j^{\downarrow}$, which shows (d). If $x_1, x_2 \in V_{j+1}$ such that $x_1 \neq x_2$, then $\psi_j^{\uparrow}\psi_j^{\downarrow}(x_1) = x_1 \neq x_2 = \psi_j^{\uparrow}\psi_j^{\downarrow}(x_2)$, which implies that $\psi_j^{\downarrow}(x_1) \neq \psi_j^{\downarrow}(x_2)$ and, therefore, $\psi_j^{\downarrow}$ is injective.

$(b),(d) \Rightarrow (a),(c)$: Recall that $(b),(d) \Rightarrow (a)$. Since $\psi_j^{\downarrow}\psi_j^{\uparrow}\psi_j^{\downarrow} = \psi_j^{\downarrow}$, we have that $\psi_j^{\downarrow}\psi_j^{\uparrow}\psi_j^{\downarrow}\psi_j^{\uparrow} = \psi_j^{\downarrow}\psi_j^{\uparrow}$, which leads to $\psi_j^{\uparrow}\psi_j^{\downarrow}\psi_j^{\uparrow} = \psi_j^{\uparrow}$, since $\psi_j^{\downarrow}$ is injective.

$(a),(c) \;\Rightarrow\; (a),(b),(e)$: This is a direct consequence of the facts that $(a),(c) \Rightarrow (b)$ and $(c) \Rightarrow (e)$.

$(a),(b),(e) \Rightarrow (f)$: From (e), we have that $\psi_j^{\downarrow}\psi_j^{\uparrow}\psi_j^{\downarrow}\psi_j^{\uparrow} = \psi_j^{\downarrow}\psi_j^{\uparrow}$ which, together with the fact that $\psi_j^{\downarrow}$ is injective, implies that $\psi_j^{\uparrow}\psi_j^{\downarrow}\psi_j^{\uparrow}(x) = \psi_j^{\uparrow}(x)$, for every $x \in V_j$. Since $\psi_j^{\uparrow}$ is surjective, $\psi_j^{\uparrow}\psi_j^{\downarrow}(y) = y$, for every $y \in V_{j+1}$. ∎

From these results, it is clear that (a)–(e) in Condition 3.1 are satisfied if and only if condition (f) is true. The latter condition plays an important role in the sequel.

3.3. Pyramid Condition. The analysis and synthesis operators $\psi_j^{\uparrow}, \psi_j^{\downarrow}$ are said to satisfy the *pyramid condition* if $\psi_j^{\uparrow}\psi_j^{\downarrow} = \mathsf{id}$ on V_{j+1}.

We now have the following proposition.

3.4. Proposition. *Assume that the pyramid condition is satisfied. Then,*

$$\psi_{i,j}^{\uparrow}\psi_{j,i}^{\downarrow} = \mathsf{id} \quad \text{on} \quad V_j, \qquad j > i \tag{3.4}$$

$$\hat{\psi}_{i,j}\hat{\psi}_{i,k} = \hat{\psi}_{i,j} = \hat{\psi}_{i,k}\hat{\psi}_{i,j}, \qquad j \geq k > i. \tag{3.5}$$

In particular, $\hat{\psi}_{i,j}$ *is idempotent.*

PROOF. From (3.1), (3.2), and the pyramid condition 3.3, we have that

$$\begin{aligned}\psi^{\uparrow}_{i,j}\psi^{\downarrow}_{j,i} &= \psi^{\uparrow}_{j-1}\psi^{\uparrow}_{j-2}\cdots\psi^{\uparrow}_{i+1}(\psi^{\uparrow}_{i}\psi^{\downarrow}_{i})\psi^{\downarrow}_{i+1}\cdots\psi^{\downarrow}_{j-1}\\ &= \psi^{\uparrow}_{j-1}\psi^{\uparrow}_{j-2}\cdots(\psi^{\uparrow}_{i+1}\psi^{\downarrow}_{i+1})\cdots\psi^{\downarrow}_{j-1}\\ &= \cdots = \psi^{\uparrow}_{j-1}\psi^{\downarrow}_{j-1} = \mathsf{id},\end{aligned}$$

which shows (3.4)

From (3.1)–(3.3) and the pyramid condition 3.3 we have that

$$\begin{aligned}\hat{\psi}_{i,j}\hat{\psi}_{i,k} &= \psi^{\downarrow}_{j,i}\psi^{\uparrow}_{i,j}\psi^{\downarrow}_{k,i}\psi^{\uparrow}_{i,k}\\ &= \psi^{\downarrow}_{i}\psi^{\downarrow}_{i+1}\cdots\psi^{\downarrow}_{j-1}\psi^{\uparrow}_{j-1}\psi^{\uparrow}_{j-2}\cdots\psi^{\uparrow}_{i+1}(\psi^{\uparrow}_{i}\psi^{\downarrow}_{i})\psi^{\downarrow}_{i+1}\cdots\psi^{\downarrow}_{k-1}\psi^{\uparrow}_{k-1}\psi^{\uparrow}_{k-2}\cdots\psi^{\uparrow}_{i}\\ &= \psi^{\downarrow}_{i}\psi^{\downarrow}_{i+1}\cdots\psi^{\downarrow}_{j-1}\psi^{\uparrow}_{j-1}\psi^{\uparrow}_{j-2}\cdots(\psi^{\uparrow}_{i+1}\psi^{\downarrow}_{i+1})\cdots\psi^{\uparrow}_{k}\psi^{\uparrow}_{k-1}\psi^{\uparrow}_{k-2}\cdots\psi^{\uparrow}_{i}\\ &= \cdots = \psi^{\downarrow}_{i}\psi^{\downarrow}_{i+1}\cdots\psi^{\downarrow}_{j-1}\psi^{\uparrow}_{j-1}\psi^{\uparrow}_{j-2}\cdots\psi^{\uparrow}_{k}(\psi^{\uparrow}_{k-1}\psi^{\downarrow}_{k-1})\psi^{\uparrow}_{k-1}\psi^{\uparrow}_{k-2}\cdots\psi^{\uparrow}_{i}\\ &= \psi^{\downarrow}_{j,i}\psi^{\uparrow}_{i,j} = \hat{\psi}_{i,j},\end{aligned}$$

which shows the first equality in (3.5). From (3.1)–(3.3) and the pyramid condition 3.3 we also have that

$$\begin{aligned}\hat{\psi}_{i,k}\hat{\psi}_{i,j} &= \psi^{\downarrow}_{k,i}\psi^{\uparrow}_{i,k}\psi^{\downarrow}_{j,i}\psi^{\uparrow}_{i,j}\\ &= \psi^{\downarrow}_{i}\psi^{\downarrow}_{i+1}\cdots\psi^{\downarrow}_{k-1}\psi^{\uparrow}_{k-1}\psi^{\uparrow}_{k-2}\cdots\psi^{\uparrow}_{i+1}(\psi^{\uparrow}_{i}\psi^{\downarrow}_{i})\psi^{\downarrow}_{i+1}\cdots\psi^{\downarrow}_{j-1}\psi^{\uparrow}_{j-1}\psi^{\uparrow}_{j-2}\cdots\psi^{\uparrow}_{i}\\ &= \cdots = \psi^{\downarrow}_{i}\psi^{\downarrow}_{i+1}\cdots\psi^{\downarrow}_{k-1}(\psi^{\uparrow}_{k-1}\psi^{\downarrow}_{k-1})\psi^{\downarrow}_{k}\psi^{\downarrow}_{k+1}\cdots\psi^{\downarrow}_{j-1}\psi^{\uparrow}_{j-1}\psi^{\uparrow}_{j-2}\cdots\psi^{\uparrow}_{i}\\ &= \psi^{\downarrow}_{j,i}\psi^{\uparrow}_{i,j} = \hat{\psi}_{i,j},\end{aligned}$$

which shows the second equality in (3.5). ∎

The first equality in (3.5) simply states that the level k approximation $\hat{\psi}_{i,k}(x)$ of a signal $x \in V_i$ is adequate for determining the level j ($j > k$) approximation $\hat{\psi}_{i,j}(x)$ of x. This agrees with our intuition that higher levels in the decomposition correspond to higher information reduction. The second equality in (3.5) says that $\hat{\psi}_{i,j}(x)$, $x \in V_i$, is not modified if approximated by means of operator $\hat{\psi}_{i,k}$.

It is worthwhile noticing here that if $V_i^{(j)} = \mathrm{Ran}(\hat{\psi}_{i,j})$ (i.e., the range of the approximation operator $\hat{\psi}_{i,j}$), then $V_i^{(j)} \subseteq V_i$ and the second equality in (3.5), with $k = j-1$, results in

$$V_i^{(j)} \subseteq V_i^{(j-1)} \subseteq V_i, \quad j > i+1. \tag{3.6}$$

Therefore, operator $\hat{\psi}_{i,j}$ decomposes the signal space V_i into nested subspaces $\cdots \subseteq V_i^{(i+2)} \subseteq V_i^{(i+1)} \subseteq V_i$, each subspace $V_i^{(j)}$ containing all "level j" ($j > i$) approximations of signals in V_i. Equation (3.6) is a basic requirement for a multiresolution signal decomposition scheme [3, 33, 16] that agrees with our intuition that the space $V_i^{(j-1)}$, which contains the approximations of signals at level i obtained by means of operator $\hat{\psi}_{i,j-1}$, contains the approximations of signals at level i obtained by means of $\hat{\psi}_{i,j}$ as well.

3.2. The pyramid transform

Although, as a direct consequence of the pyramid condition 3.3, the analysis operator $\psi_j^{\uparrow}$ is the left inverse of the synthesis operator $\psi_j^{\downarrow}$, it is not true in general that is also the right inverse: $\psi_j^{\downarrow}\psi_j^{\uparrow}(x)$ is only an approximation of $x \in V_j$. Therefore, the analysis step cannot be used by itself for signal representation. This is not a problem however. In fact, this is in agreement with the inherent property of multiresolution signal decomposition of reducing information in the direction of increasing j.

Analysis of a signal $x \in V_j$, followed by synthesis, yields an approximation $\hat{x} = \hat{\psi}_{j,j+1}(x) = \psi_j^{\downarrow}\psi_j^{\uparrow}(x) \in \hat{V}_j$ of x, where $\hat{V}_j = V_j^{(j+1)}$. We assume here that there exists a *subtraction operator* $(x, \hat{x}) \mapsto x \dot{-} \hat{x}$ mapping $V_j \times \hat{V}_j$ into a set Y_j (strictly speaking, we should write $\dot{-}_j$ to denote dependence on level j). Furthermore, we assume that there exists an *addition operator* $(\hat{x}, y) \mapsto \hat{x} \dot{+} y$ mapping $\hat{V}_j \times Y_j$ into V_j. The *detail signal* $y = x \dot{-} \hat{x}$ contains information about x which is not present in $\hat{x}$. It is crucial that x can be reconstructed from its approximation $\hat{x}$ and the detail signal y. Towards this goal, we introduce the following assumption of *perfect reconstruction*:

$$\hat{x} \dot{+} (x \dot{-} \hat{x}) = x, \quad \text{if } x \in V_j \ \text{ and } \hat{x} = \hat{\psi}_{j,j+1}(x). \tag{3.7}$$

This leads to the following recursive signal analysis scheme:

$$x \to \{y_0, x_1\} \to \{y_0, y_1, x_2\} \to \cdots \to \{y_0, y_1, \ldots, y_j, x_{j+1}\} \to \cdots \tag{3.8}$$

where

$$\begin{cases} x_0 = x \in V_0 \\ x_{j+1} = \psi_j^{\uparrow}(x_j) \in V_{j+1}, \quad j \geq 0 \ . \\ y_j = x_j \dot{-} \psi_j^{\downarrow}(x_{j+1}) \in Y_j \end{cases} \tag{3.9}$$

Notice that, because of the perfect reconstruction condition, signal $x \in V_0$ can be *exactly* reconstructed from x_{j+1} and $y_0, y_1, \ldots, y_j$ by means of the backward recursion

$$x = x_0, \ x_j = \psi_j^{\downarrow}(x_{j+1}) \dot{+} y_j, \ j \geq 0. \tag{3.10}$$

3.5. Example. The specific choice for the subtraction and addition operators depends upon the application at hand. Below, we discuss three alternatives for which the perfect reconstruction condition holds. In all cases, we assume that our signals lie in $\text{Fun}(E, \mathcal{T})$, for some gray-value set $\mathcal{T}$. Now, it suffices to define subtraction and addition operators on $\mathcal{T}$.

(*a*) Assume that $\mathcal{T} \subseteq \mathbb{R}$ and let $\mathcal{T}' = \{t - s \mid t, s \in \mathcal{T}\}$. We define a subtraction operator $(t, s) \mapsto t - s$ from $\mathcal{T} \times \mathcal{T}$ into $\mathcal{T}'$. Obviously, the perfect reconstruction condition is valid if we choose the standard addition $+$ as the addition operator.

(*b*) Suppose that $\mathcal{T}$ is a complete lattice. If we know that the approximation signal $\hat{x}$ satisfies $\hat{x} \leq x$ pointwise (see Section 5 for examples), then we can define

$$t \dot{-} s = \begin{cases} t, & \text{if } t > s \\ \bot, & \text{if } t = s \ , \end{cases} \tag{3.11}$$

where $\bot$ is the least element of $\mathcal{T}$. For $\dot{+}$ we simply take

$$t \dot{+} s = t \vee s. \tag{3.12}$$

It is easy to verify that $s \dot{+} (t \dot{-} s) = t$, for every $t, s \in \mathcal{T}$ with $s \leq t$.

(*c*) Assume that $\mathcal{T}$ is finite, say $\mathcal{T} = \{0, 1, \ldots, N-1\}$. Define $\dot{+}$ and $\dot{-}$ as the addition and subtraction in the Abelian group $\mathbb{Z}_N$; i.e., $t \dot{+} s = (t+s) \bmod N$ and $t \dot{-} s = (t-s) \bmod N$, where 'mod' denotes *modulo*. Observe that in the binary case, both $\dot{+}$ and $\dot{-}$ correspond to the 'exclusive OR' operator. ∎

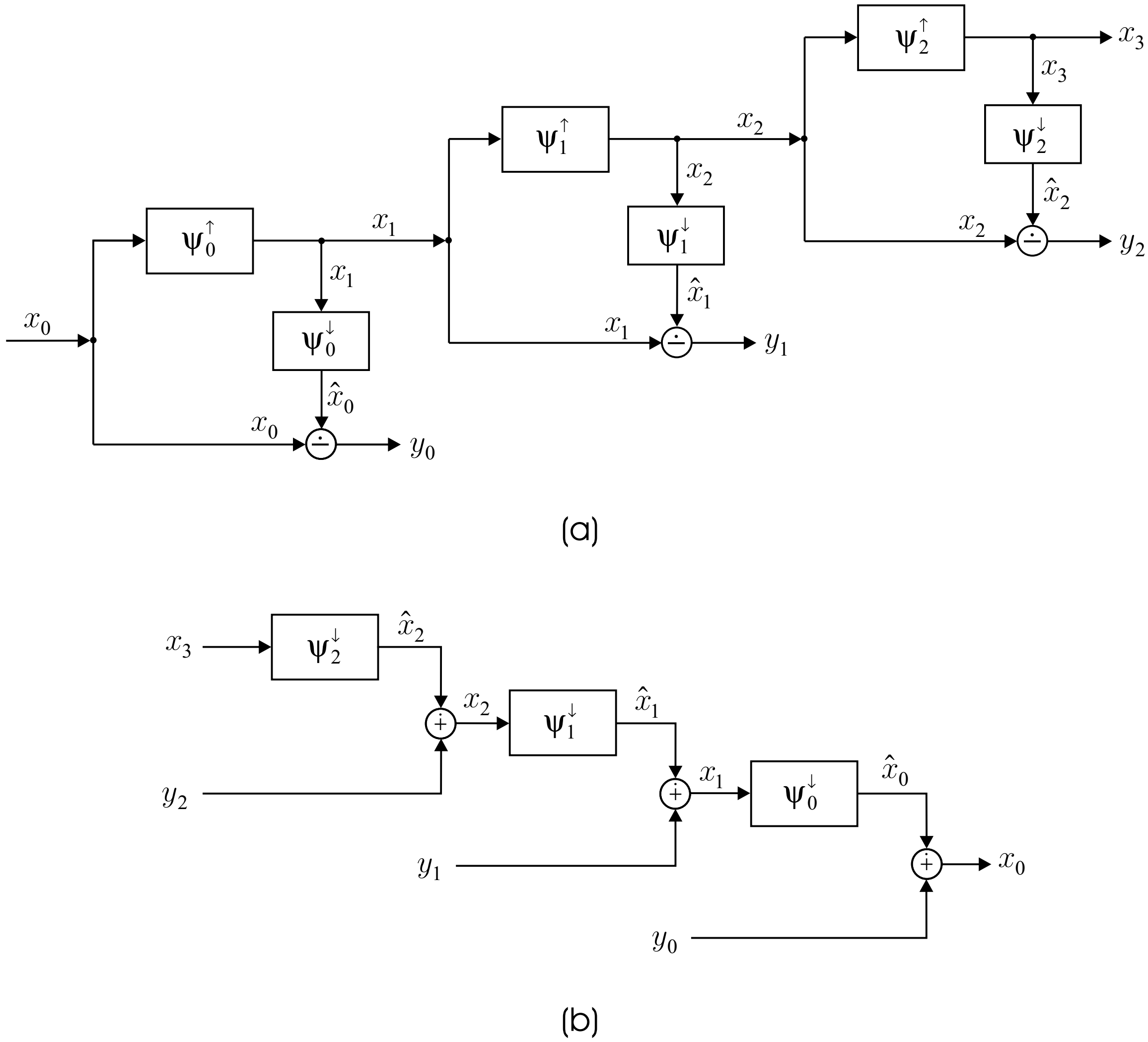

Fig. 1. Illustration of: (a) a 3-level pyramid transform, and (b) its inverse.

In the definition below, we use the following notation:

$$\bar{J} = \begin{cases} J \cup \{K+1\}, \text{ if } J = \{0, 1, \ldots, K\} \\ J, \text{ if } J = \{0, 1, \ldots\}. \end{cases}$$

3.6. Definition. Consider the multiresolution signal decomposition scheme given by J, $(V_j)_{j \in \bar{J}}$, $(\psi_j^{\uparrow})_{j \in J}$, $(\psi_j^{\downarrow})_{j \in J}$. The process of decomposing a signal $x \in V_0$ in terms of (3.8), (3.9) is called the *pyramid transform* (PT) of x, whereas the process of synthesizing x by means of (3.10) is called the *inverse pyramid transform* (IPT).

Block diagrams illustrating the pyramid transform and its inverse, for the case when $J = \{0, 1, 2\}$, are depicted in Figure 1.

3.3. An elementary sampling scheme

In most of the examples to follow, it is assumed that the domains V_j coincide and that operators $\psi_j^{\uparrow}$ and $\psi_j^{\downarrow}$ are the same at each level. Here, we discuss one of the most elementary examples of a pyramid transform for the case when $V_j = \mathrm{Fun}(\mathbb{Z}^d, \mathcal{T})$, with $\mathcal{T}$ being an arbitrary set. Let $t \in \mathcal{T}$ be a fixed value and consider the operators

$$\sigma^{\uparrow}(x)(n) = x(2n)$$
$$\sigma_t^{\downarrow}(x)(2n) = x(n) \quad \text{and} \quad \sigma_t^{\downarrow}(x)(m) = t, \text{ if } m \notin 2\mathbb{Z}^d,$$

where $2\mathbb{Z}^d$ denotes all vectors in $\mathbb{Z}^d$ with *even* coordinates. It is easy to see that $\sigma^{\uparrow}\sigma_t^{\downarrow} = \mathsf{id}$ on $\mathrm{Fun}(\mathbb{Z}^d, \mathcal{T})$, which means that the pyramid condition 3.3 holds.

If $\mathcal{T}$ is a linear space and we choose $t = 0$, then both $\sigma^{\uparrow}$ and $\sigma_0^{\downarrow}$ are linear operators. The case when $\mathcal{T}$ is a complete lattice is governed by the following result.

3.7. Proposition. *Assume that $\mathcal{T}$ is a complete lattice, with least element $\perp$ and greatest element $\top$. Then $(\sigma^{\uparrow}, \sigma_{\perp}^{\downarrow})$ and $(\sigma_{\top}^{\downarrow}, \sigma^{\uparrow})$ are both adjunctions on* $\mathrm{Fun}(\mathbb{Z}^d, \mathcal{T})$.

The proof of this result is straightforward.

4. Linear Pyramids

A case of particular interest to signal processing and analysis applications is when the analysis/synthesis operators are linear and translation invariant. In this section, we provide a number of (known as well as new) examples associated with linear translation invariant pyramids. First, we consider the case of pyramids which successively reduce the number of data points (samples) at each level. Since sample reduction results in scale reduction as well [33], we refer to these pyramids as *multiscale pyramids*. We then discuss the case of linear translation invariant pyramids with no sample reduction. We refer to these pyramids as *single-scale pyramids*.

4.1. Multiscale pyramids

4.1.1. The one-dimensional case

In this subsection, we restrict attention to one-dimensional discrete-time signals x, viewed as elements in $\ell^2(\mathbb{Z})$, the space of all real-valued sequences on $\mathbb{Z}$ which are square summable. Let τ be the translation operator on $\ell^2(\mathbb{Z})$, for which

$$(\tau x)(n) = x(n-1) \quad \text{and} \quad (\tau^{-1}x)(n) = x(n+1),$$

where τ^{-1} is the inverse of τ. We consider pyramid transforms satisfying the following assumptions:

(*i*) All domains V_j are identical, namely $\ell^2(\mathbb{Z})$.

(*ii*) Operators $\dot{+}$ and $\dot{-}$ are the usual addition and difference operators $+$ and $-$ in the linear space $\ell^2(\mathbb{Z})$.

(*iii*) At every level j, we use the same analysis and synthesis operators, i.e., $\psi_j^{\uparrow}$ and $\psi_j^{\downarrow}$ are independent of j; they are denoted by $\psi^{\uparrow}$ and $\psi^{\downarrow}$, respectively.

(*iv*) $\psi^{\uparrow}$ and $\psi^{\downarrow}$ are linear operators.

(*v*) $\psi^{\uparrow}$ and $\psi^{\downarrow}$ are translation invariant in the following sense:

$$\psi^{\uparrow}\tau^2 = \tau\psi^{\uparrow} \quad \text{and} \quad \psi^{\downarrow}\tau = \tau^2\psi^{\downarrow}. \tag{4.1}$$

A straightforward computation shows that there exist *convolution kernels* $\tilde{h}, h \in \ell^2(\mathbb{Z})$ such that $\psi^\uparrow$ and $\psi^\downarrow$ are of the following general form (see Rioul [26]):

$$\psi^\uparrow(x)(n) = \sum_{k=-\infty}^{\infty} \tilde{h}(2n-k)x(k) \tag{4.2}$$

$$\psi^\downarrow(x)(n) = \sum_{k=-\infty}^{\infty} h(n-2k)x(k). \tag{4.3}$$

Note that the analysis operator $\psi^\uparrow$ can be regarded as a linear convolution with kernel $\tilde{h}$ followed by a downsampling at rate 2. The pyramid condition $\psi^\uparrow\psi^\downarrow = \mathsf{id}$ amounts to

$$\sum_{k=-\infty}^{\infty} \tilde{h}(2n-k)h(k) = \delta(n), \tag{4.4}$$

where $\delta(n)$ is the *Dirac-delta sequence*; i.e., $\delta(0) = 1$ and $\delta(n) = 0$, if $n \neq 0$. This is known as the *biorthogonality condition* [26].

4.1. Example (Haar pyramid). A simple solution to (4.4) is

$$\begin{cases} \tilde{h}(-1) = \tilde{h}(0) = \frac{1}{2} \text{ and } \tilde{h}(n) = 0, \text{ otherwise} \\ h(0) = h(1) = 1 \text{ and } h(n) = 0, \text{ otherwise,} \end{cases}$$

which corresponds to the analysis and synthesis operators

$$\psi^\uparrow(x)(n) = \frac{1}{2}(x(2n) + x(2n+1)) \tag{4.5}$$

$$\psi^\downarrow(x)(2n) = \psi^\downarrow(x)(2n+1) = x(n). \tag{4.6}$$

This leads to a signal decomposition scheme which we call the *Haar pyramid*; the operators in (4.5), (4.6) coincide with the lowpass filters associated with the Haar wavelet [3, 33, 30] ∎

4.2. Example (Burt–Adelson pyramid). We may set

$$\begin{cases} \tilde{h}(0) = a, \quad \tilde{h}(-1) = \tilde{h}(1) = b, \quad \tilde{h}(-2) = \tilde{h}(2) = c, \quad \tilde{h}(n) = 0, \text{ otherwise} \\ h(0) = p, \quad h(-1) = h(1) = q, \quad h(n) = 0, \text{ otherwise.} \end{cases}$$

Condition (4.4) gives rise to the following equations:

$$2bq + ap = 1 \text{ and } cp + bq = 0.$$

If we impose two normalizing conditions, namely that $\psi^\uparrow$ maps signal $(\ldots, 1, -1, 1, -1, 1, \ldots)$ to $(\ldots, 0, 0, 0, 0, 0, \ldots)$, whereas $\psi^\downarrow$ maps signal $(\ldots, 1, 1, 1, 1, 1, \ldots)$ to itself, we get

$$a - 2b + 2c = 0 \text{ and } p = 2q = 1.$$

The *unique* solution to these equations is

$$a = \frac{3}{4}, \ b = \frac{1}{4}, \ c = -\frac{1}{8}, \ p = 1, \ q = \frac{1}{2},$$

which corresponds to the analysis and synthesis operators

$$\psi^\uparrow(x)(n) = \frac{1}{8}(-x(2n-2) + 2x(2n-1) + 6x(2n) + 2x(2n+1) - x(2n+2))$$

$$\psi^\downarrow(x)(2n) = x(n) \quad \text{and} \quad \psi^\downarrow(x)(2n+1) = \frac{1}{2}(x(n) + x(n+1)).$$

This leads to a signal decomposition scheme which is a particular case of the well-known *Burt–Adelson pyramid* [1]. ∎

It is clear from (4.2) and (4.3) that the analysis operator reduces the number of samples by a factor of two whereas the synthesis operator doubles the number of samples. Therefore, a signal $x \in V_0$ of 2^K samples is reduced to a signal $\psi^{\uparrow}(x) \in V_1$ of 2^{K-1} samples, which is then expanded to a signal $\psi^{\downarrow}\psi^{\uparrow}(x) \in \hat{V}_0$ of 2^K samples. If we consider a pyramid transform $\{y_0, y_1, \ldots, y_{K-1}, x_K\}$, it is not difficult to see that signal x_K contains 1 sample, whereas the detail signal y_j contains 2^{K-j} samples. Therefore, the pyramid transform of a signal $x \in V_0$ of 2^K samples contains $1+2+2^2+\cdots+2^K = 2^{K+1}-1$ samples, an increase by a factor of $(2^{K+1}-1)/2^K \to 2$, as $K \to \infty$. Hence, the pyramid transform is an *overcomplete* signal decomposition, since it produces more information than is actually needed for signal representation.

4.1.2. The 2-dimensional case

It is straightforward to generalize the previous result to the 2-dimensional case. We make the same assumptions (i)–(v) as before; however, the translation invariance condition in (4.1) should hold for every translation operator $\tau = \tau_{(k,l)}$, given by $(\tau_{(k,l)}x)(m,n) = x(m-k, n-l)$. It can be shown that there exist convolution kernels $\tilde{h}, h \in \ell^2(\mathbb{Z}^2)$ such that $\psi^{\uparrow}, \psi^{\downarrow}$ are given by

$$\begin{aligned}(\psi^{\uparrow}x)(m,n) &= \sum_{k,l=-\infty}^{\infty} \tilde{h}(2m-k, 2n-l)x(k,l)\\ \psi^{\downarrow}(x)(m,n) &= \sum_{k,l=-\infty}^{\infty} h(m-2k, n-2l)x(k,l).\end{aligned}$$

The pyramid condition $\psi^{\uparrow}\psi^{\downarrow} = \mathsf{id}$ amounts to the identity

$$\sum_{k,l=-\infty}^{\infty} \tilde{h}(2m-k, 2n-l)h(k,l) = \delta(m,n), \tag{4.7}$$

where δ is the 2-dimensional Dirac-delta sequence, given by $\delta(m,n) = 1$, if $m = n = 0$, and 0 otherwise.

The simplest solution to (4.7) is similar to the Haar decomposition given in Example 4.1:

$$\begin{cases}\tilde{h}(-1,-1) = \tilde{h}(-1,0) = \tilde{h}(0,-1) = \tilde{h}(0,0) = \frac{1}{4} \text{ and } \tilde{h}(m,n) = 0, \text{ otherwise}\\ h(0,0) = h(1,0) = h(0,1) = h(1,1) = 1 \text{ and } h(m,n) = 0, \text{ otherwise .}\end{cases}$$

The following example discusses a less trivial solution.

4.3. Example. Let us consider the case when, in the analysis step, a 2×2 pixel block $\{(2m,2n), (2m+1,2n), (2m+1,2n+1), (2m,2n+1)\}$ at level j is replaced by one pixel (m,n) at level $j+1$. The value of this pixel is a weighted average over 16 pixels at level j, namely the pixels in the 4×4 block surrounding the 2×2 block; see Figure 2. To be precise:

$$\begin{aligned}\psi^{\uparrow}(x)(m,n) = a\big(&x(2m,2n) + x(2m+1,2n) + x(2m+1,2n+1) + x(2m,2n+1)\big)\\ +b\big(&x(2m-1,2n) + x(2m-1,2n+1) + x(2m,2n-1) + x(2m+1,2n-1)\\ &+x(2m+2,2n) + x(2m+2,2n+1) + x(2m,2n+2) + x(2m+1,2n+2)\big)\\ +c\big(&x(2m-1,2n-1) + x(2m+2,2n-1) + x(2m+2,2n+2) + x(2m-1,2n+2)\big).\end{aligned} \tag{4.8}$$

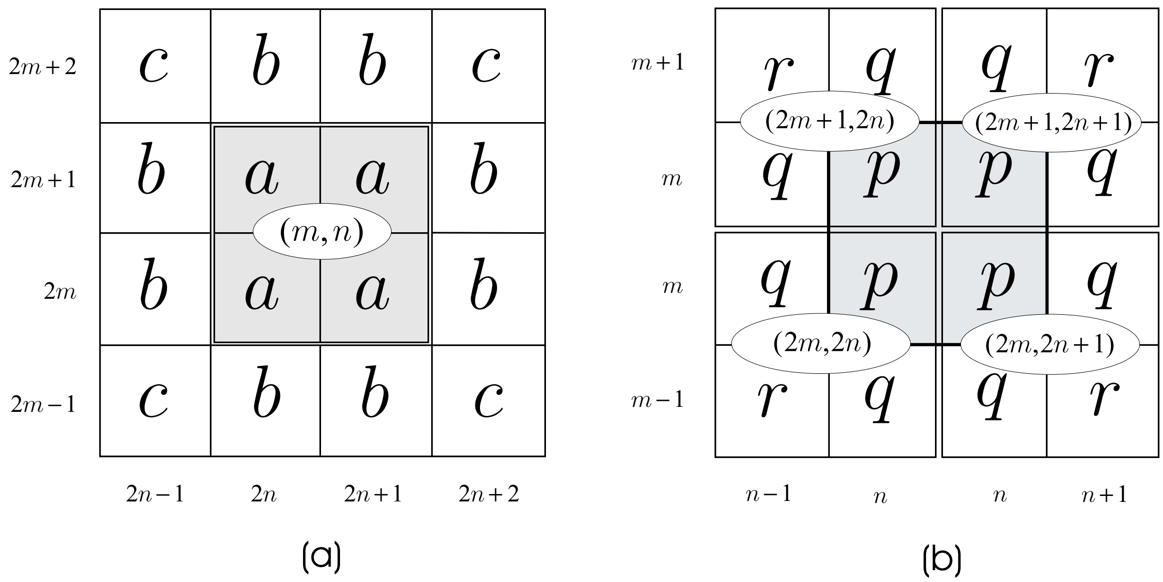

Fig. 2. Stencils for: (a) $\psi^{\uparrow}$ in (4.8), and (b) $\psi^{\downarrow}$ in (4.9)–(4.12).

The synthesis step subdivides a pixel (m,n) at level $j+1$ into 4 pixels $\{(2m,2n),(2m+1,2n),(2m+1,2n+1),(2m,2n+1)\}$ at level j. The values of $\psi^{\downarrow}(x)$ are given by (see Figure 2)

$$\psi^{\downarrow}(x)(2m,2n) = px(m,n) + q(x(m-1,n) + x(m,n-1)) + rx(m-1,n-1) \tag{4.9}$$
$$\psi^{\downarrow}(x)(2m+1,2n) = px(m,n) + q(x(m+1,n) + x(m,n-1)) + rx(m+1,n-1) \tag{4.10}$$
$$\psi^{\downarrow}(x)(2m,2n+1) = px(m,n) + q(x(m,n+1) + x(m-1,n)) + rx(m-1,n+1) \tag{4.11}$$
$$\psi^{\downarrow}(x)(2m+1,2n+1) = px(m,n) + q(x(m+1,n) + x(m,n+1)) + rx(m+1,n+1). \tag{4.12}$$

The pyramid condition (4.7) leads to the following relations

$$\begin{aligned} &4ap + 8bq + 4cr = 1 \\ &2aq + 2bp + 2br + 2cq = 0 \\ &ar + 2bq + cp = 0. \end{aligned}$$

It is obvious that, due to the symmetry in $\tilde{h}$, $\psi^{\uparrow}$ maps the high-frequency signals $x(m,n) = (-1)^m$, $(-1)^n$, $(-1)^{m+n}$ onto the zero signal. We impose the following two normalizing conditions: $\psi^{\uparrow}$ and $\psi^{\downarrow}$ map a constant signal onto the same constant signal (albeit at a different level of the pyramid). This yields the following two conditions:

$$\begin{aligned} &4a + 8b + 4c = 1 \\ &p + 2q + r = 1. \end{aligned}$$

The *unique* solution of the previous system of 5 equations with 6 unknowns can be expressed in terms of a as:

$$b = a, \quad c = \frac{1}{4} - 3a, \quad p = q = \frac{4a}{16a-1}, \quad r = \frac{4a-1}{16a-1}.$$

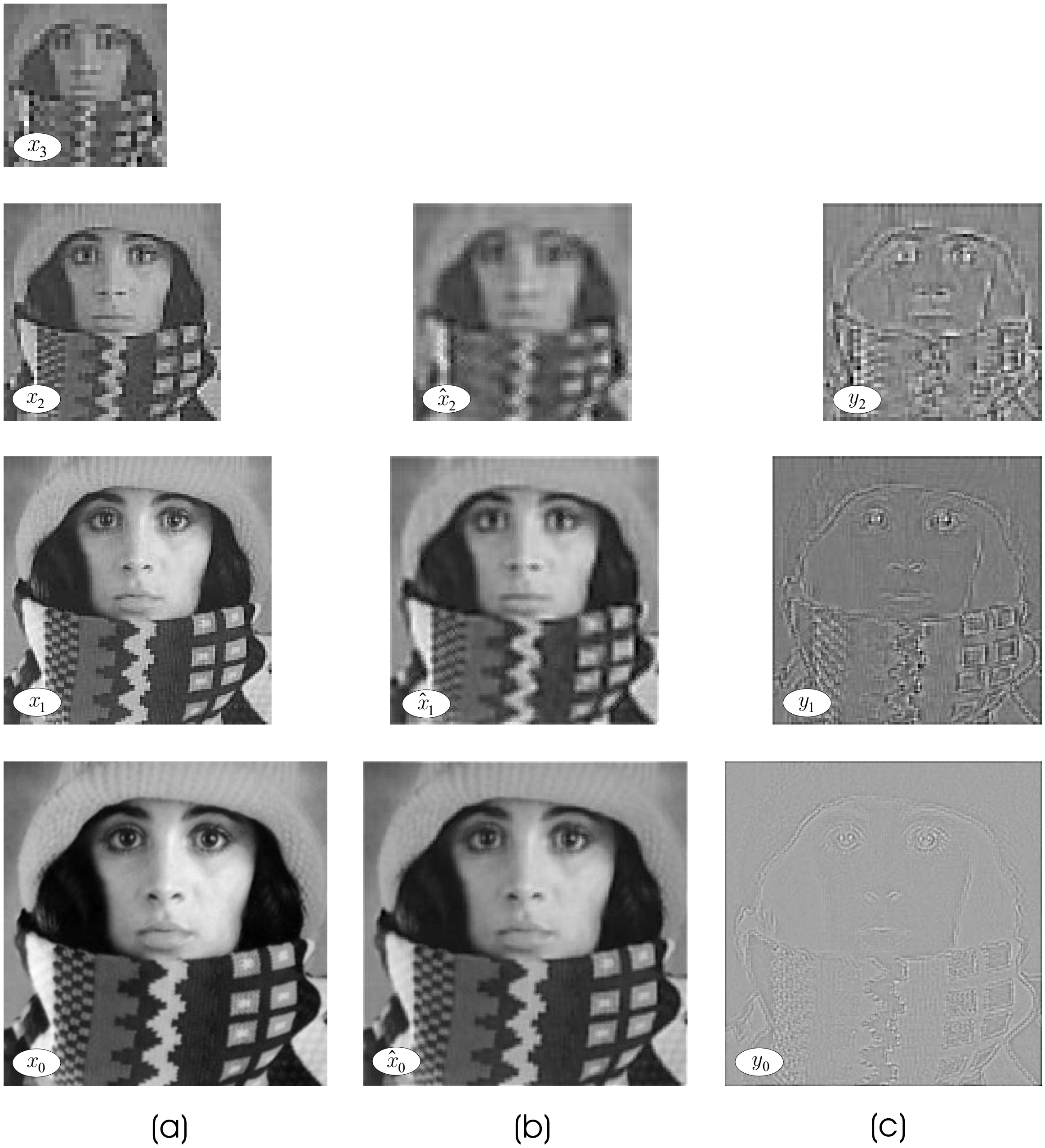

Fig. 3. Multiresolution image decomposition based on the linear pyramid transform of Example 4.3: (a) An image x_0 and its decomposition $\{x_0, x_1, x_2, x_3\}$ obtained by means of the analysis operator $\psi^{\uparrow}$ in (4.8), where a, b, c are given by (4.13). (b) The approximation images $\{\hat{x}_0, \hat{x}_1, \hat{x}_2\}$ obtained from $\{x_1, x_2, x_3\}$ by means of the synthesis operator $\psi^{\downarrow}$ in (4.9)–(4.12), where p, q, r are given by (4.13). (c) The detail images $\{y_0, y_1, y_2\}$.

Clearly, we must exclude $a = \frac{1}{16}$ in order to avoid singularities. When $a = 1/4$, then

$$a = b = \frac{1}{4}, \quad c = -\frac{1}{2}, \quad p = q = \frac{1}{3}, \quad r = 0. \tag{4.13}$$

An example, illustrating the resulting linear pyramid, is depicted in Figure 3. Due to the calculations associated with (4.8)–(4.12), the resulting images will not have integer gray-values between 0 and 255, as required for computer storage and display, even if the original image is already quantized to these values. To comply with this requirement, all gray-values of the images depicted in Figure 3 have been mapped to integers between 0 and 255, with the minimum and maximum values being mapped to 0 and 255, respectively. Finally, and for clarity of presentation, the size of some of the images depicted in Figure 3 (and later in this report) is larger than their actual size (e.g., although the size of x_1 should be half the size of x_0, this is not the case in Figure 3).

It is worthwhile noticing here that most of the linear pyramid transforms used in the literature are one-dimensional. These transforms, when applied on images, use *separable* analysis and synthesis operators. The linear pyramid transform discussed in this example employs non-separable analysis and synthesis operators. It is, therefore, an example of a pure (non-separable) 2-dimensional linear pyramid transform. ∎

4.2. Single-scale pyramids

In the case of single-scale pyramids, no sample reduction takes place and the pyramid performs multiresolution signal decomposition by successively applying linear filtering. In this subsection, we consider pyramid transforms satisfying the following assumptions:

(i) All domains V_j are linear subspaces of $\ell^2(\mathbb{Z})$.

(ii) Operators $\dot{+}$ and $\dot{-}$ are the usual addition and difference operators $+$ and $-$ in the linear space $\ell^2(\mathbb{Z})$.

(iii) $\psi_j^{\uparrow}$ and $\psi_j^{\downarrow}$ are linear operators.

(iv) $\psi_j^{\uparrow}$ and $\psi_j^{\downarrow}$ are translation invariant in the classical sense:

$$\psi_j^{\uparrow}\tau = \tau\psi_j^{\uparrow} \quad \text{and} \quad \psi_j^{\downarrow}\tau = \tau\psi_j^{\downarrow}.$$

Furthermore, assuming that the analysis and synthesis operators depend on the level j in the pyramid, we get

$$\psi_j^{\uparrow}(x)(n) = (\tilde{h}_j * x)(n) = \sum_{k=-\infty}^{\infty} \tilde{h}_j(n-k)x(k)$$
$$\psi_j^{\downarrow}(x)(n) = (h_j * x)(n) = \sum_{k=-\infty}^{\infty} h_j(n-k)x(k),$$

where $\tilde{h}_j, h_j \in \ell^2(\mathbb{Z})$ are convolution kernels. For an element $x \in \ell^2(\mathbb{Z})$, we denote its Fourier transform by $X(\omega)$, where $\omega \in (-\pi, \pi]$. Let $x_0 \in V_0$ be a given input signal. The Fourier transform of the reduced signal $x_j = \psi_{0,j}^{\uparrow}(x_0) = \psi_{j-1}^{\uparrow}\psi_{j-2}^{\uparrow}\cdots\psi_0^{\uparrow}(x_0)$ at level j is given by

$$X_j(\omega) = \tilde{H}_{j-1}(\omega)\tilde{H}_{j-2}(\omega)\cdots\tilde{H}_0(\omega)X_0(\omega).$$

We now define V_j in the following way:

$$V_j = \{x \in \ell^2(\mathbb{Z}) \mid X(\omega) = \tilde{H}_{j-1}(\omega)\tilde{H}_{j-2}(\omega)\cdots\tilde{H}_0(\omega)X_0(\omega), \text{ for some } x_0 \in \ell^2(\mathbb{Z})\}.$$

Denote by $z(\tilde{H}_j)$ the *zero set* of $\tilde{H}_j$, i.e.

$$z(\tilde{H}_j) = \{\omega \in (-\pi, \pi] \mid \tilde{H}_j(\omega) = 0\}.$$

It is evident that, if $x \in V_j$, then $X(\omega) = 0$ on

$$\Omega_j := z(\tilde{H}_0) \cup z(\tilde{H}_1) \cup \cdots \cup z(\tilde{H}_{j-1}).$$

In the frequency domain, the pyramid condition $\psi_j^{\uparrow}\psi_j^{\downarrow} = \mathsf{id}$ on V_{j+1} amounts to

$$\tilde{H}_j(\omega)H_j(\omega)\tilde{H}_j(\omega)\tilde{H}_{j-1}(\omega)\cdots\tilde{H}_0(\omega) = \tilde{H}_j(\omega)\tilde{H}_{j-1}(\omega)\cdots\tilde{H}_0(\omega),$$

which is equivalent to

$$\tilde{H}_j(\omega)H_j(\omega) = 1, \quad \text{for } \omega \notin \Omega_{j+1}. \tag{4.14}$$

We put $\hat{x}_j = \psi_j^{\downarrow}\psi_j^{\uparrow}(x_j)$ and $y_j = x_j - \hat{x}_j$. A straightforward calculation shows that

$$\begin{cases} \hat{X}_j(\omega) = X_j(\omega) \text{ and } Y_j(\omega) = 0, & \text{for } \omega \notin \Omega_{j+1} \\ \hat{X}_j(\omega) = 0 \text{ and } Y_j(\omega) = X_j(\omega), & \text{for } \omega \in \Omega_{j+1} \end{cases}.$$

Notice that the set Ω_j becomes larger when j increases. For Y_j we can also write

$$Y_0(\omega) = \Big(1 - H_0(\omega)\tilde{H}_0(\omega)\Big)X_0(\omega) \tag{4.15}$$

$$Y_j(\omega) = \Big(1 - H_j(\omega)\tilde{H}_j(\omega)\Big)\tilde{H}_{j-1}(\omega)\tilde{H}_{j-2}(\omega)\cdots\tilde{H}_0(\omega)X_0(\omega), \quad \text{for } j \geq 1. \tag{4.16}$$

Equations (4.14)–(4.16) show that, when $\tilde{h}_j$ is the impulse response of a low-pass filter, the detail signal y_j is the output of an *unsharp masking* operator [5], based on an ideal low-pass filter, to input $(\tilde{h}_{j-1} * \tilde{h}_{j-2} * \cdots * \tilde{h}_0) * x_0$. Therefore, single-scale linear pyramids produce a multiresolution unsharp masking signal decomposition. Notice that, in this case, y_j is obtained from x_j through an ideal high-pass filter, since $Y_j(\omega) = (1 - H_j(\omega)\tilde{H}_j(\omega))X_j(\omega)$.

If, for some $j \geq 0$, we have that $\Omega_{j+1} = \Omega_j$, that is $z(\tilde{H}_j) \subseteq \Omega_j$, then we find that $\hat{X}_j = X_j$ and $Y_j = 0$, which means that the analysis step $\psi_{j+1}^{\uparrow}$ does not reduce the data in x_j. Therefore, the analysis operators of a multilevel linear single-scale pyramid should be different at each level. Finally, the previous discussion can be extended to the 2-dimensional case in a straightforward manner. We now have the following example.

4.4. Example. Consider a 2-dimensional linear single-scale pyramid, with $\tilde{h}_j$ being a 2-dimensional Gaussian convolution kernel, given by

$$\tilde{h}_j(m,n) = \frac{e^{-(m^2+n^2)/2\pi\sigma_j^2}}{\sum_k \sum_l e^{-(k^2+l^2)/2\pi\sigma_j^2}}, \tag{4.17}$$

where

$$\sigma_{j+1} = 2\sigma_j. \tag{4.18}$$

Figure 4 illustrates four levels of the resulting single-scale pyramid, for the case when $\sigma_0 = 3$. Notice the strong ripple effect present in the detail images, which is a direct consequence of the fact that the detail image y_j is obtained from x_j by means of an *ideal* high-pass filter. ∎

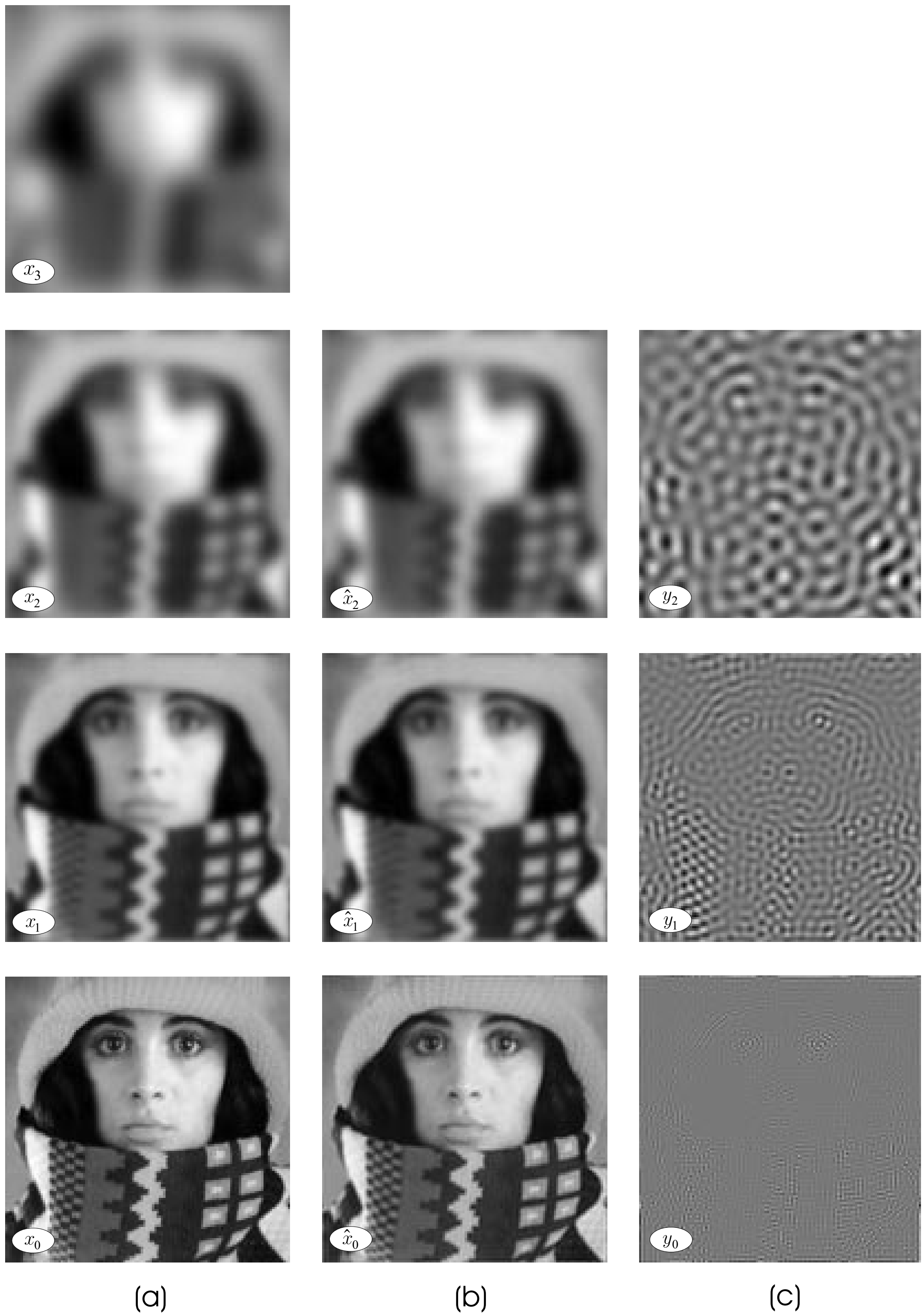

Fig. 4. Multiresolution image decomposition based on the linear pyramid transform of Example 4.4: (a) An image x_0 and its decomposition $\{x_0, x_1, x_2, x_3\}$ obtained by means of a linear analysis operator, with convolution kernel $\tilde{h}_j$ given by (4.17), where σ_j is given by (4.18), with $\sigma_0 = 3$. (b) The approximation images $\{\hat{x}_0, \hat{x}_1, \hat{x}_2\}$ obtained from $\{x_1, x_2, x_3\}$ by means of the composed filter $\hat{x}_j = h_j * \tilde{h}_j * x_j$. (c) The detail images $\{y_0, y_1, y_2\}$.

5. Morphological Adjunction Pyramids

As we have previously observed, the pyramid condition 3.3 is the only condition to be imposed on a multiresolution scheme. There is no a priori reason why the operators involved should be translation invariant and/or linear. In this section, we consider the special, but interesting, case when the signal domains are complete lattices and the analysis and synthesis operators between two adjacent levels in the pyramid form an adjunction. More precisely, we make the following assumptions:

(*i*) All domains V_j have the structure of a complete lattice.
(*ii*) The pair $(\psi_j^{\uparrow}, \psi_j^{\downarrow})$ is an adjunction between V_j and V_{j+1}.

In this case, $\psi_j^{\uparrow}$ is an erosion and $\psi_j^{\downarrow}$ is a dilation. From the standard theory of adjunctions (see Section 2) we know that (c)–(e) in Condition 3.1 are satisfied. From Proposition 3.2, it is clear that the pyramid condition is satisfied if and only if $\psi_j^{\downarrow}$ is injective, or, alternatively, if $\psi_j^{\uparrow}$ is surjective. Notice that $\psi_j^{\downarrow}\psi_j^{\uparrow}$ is an opening and hence $\psi_j^{\downarrow}\psi_j^{\uparrow} \leq \mathsf{id}$; i.e., the approximation operator $\psi_j^{\downarrow}\psi_j^{\uparrow}$ is anti-extensive.

As we did in the linear case, we distinguish between two types of pyramids: those ones that involve sample reduction (i.e., multiscale pyramids) and those ones that do not (i.e., single-scale pyramids).

5.1. Multiscale pyramids

5.1.1. Representation

In this subsection, we give a complete characterization of analysis and synthesis operators, between two adjacent levels $j = 0$ and $j = 1$ in a pyramid, under the following general assumptions:

1. $V_0 = V_1 = \mathrm{Fun}(\mathbb{Z}^d, \mathcal{T})$, the complete lattice of functions from $\mathbb{Z}^d$ into a given complete lattice $\mathcal{T}$ of gray-values.
2. The analysis operator $\psi^{\uparrow}\colon V_0 \to V_1$ and the synthesis operator $\psi^{\downarrow}\colon V_1 \to V_0$ form an adjunction between V_0 and V_1; i.e.,

$$x_1 \leq \psi^{\uparrow}(x_0) \iff \psi^{\downarrow}(x_1) \leq x_0, \quad x_0 \in V_0,\ x_1 \in V_1.$$

3. For every translation $\tau = \tau_{(k_1,k_2,\ldots,k_d)}$ of $\mathbb{Z}^d$, we have that

$$\psi^{\uparrow}\tau^2 = \tau\psi^{\uparrow} \quad \text{and} \quad \psi^{\downarrow}\tau = \tau^2\psi^{\downarrow}. \tag{5.1}$$

Our characterization is given in terms of adjunctions (e, d) on the complete lattice $\mathcal{T}$ and is closely related to the representation of translation invariant adjunctions for grayscale functions in mathematical morphology [11, 7].

5.1. Proposition. *Let $(\psi^{\uparrow}, \psi^{\downarrow})$ be an adjunction on $\mathrm{Fun}(\mathbb{Z}^d, \mathcal{T})$. The translation invariance condition $\psi^{\uparrow}\tau^2 = \tau\psi^{\uparrow}$ implies that $\psi^{\downarrow}\tau = \tau^2\psi^{\downarrow}$ and vice versa. Every adjunction satisfying these equivalent conditions is of the form*

$$\psi^{\uparrow}(x)(n) = \bigwedge_{k\in\mathbb{Z}^d} e_{k-2n}(x(k)) \tag{5.2}$$

$$\psi^{\downarrow}(x)(k) = \bigvee_{n\in\mathbb{Z}^d} d_{k-2n}(x(n)), \tag{5.3}$$

where (e_k, d_k) defines an adjunction on $\mathcal{T}$, for every $k \in \mathbb{Z}^d$.

Proof. We show the first part of the assertion concerning translation invariance; the other implication is proved analogously. Assume that $\psi^{\uparrow}\tau^2 = \tau\psi^{\uparrow}$, for every translation τ. For $x_0, x_1 \in \mathrm{Fun}(\mathbb{Z}^d, \mathcal{T})$, we have the following equivalences:

$$\begin{aligned}
\psi^{\downarrow}\tau(x_1) \le x_0 &\iff \tau(x_1) \le \psi^{\uparrow}(x_0) \\
&\iff x_1 \le \tau^{-1}\psi^{\uparrow}(x_0) \\
&\iff x_1 \le \psi^{\uparrow}\tau^{-2}(x_0) \\
&\iff \psi^{\downarrow}(x_1) \le \tau^{-2}(x_0) \\
&\iff \tau^2\psi^{\downarrow}(x_1) \le x_0.
\end{aligned}$$

This yields that $\psi^{\downarrow}\tau = \tau^2\psi^{\downarrow}$.

We next prove the identities in (5.2) and (5.3). From [7, Prop. 5.3] it follows that every adjunction $(\psi^{\uparrow}, \psi^{\downarrow})$ on $\mathrm{Fun}(\mathbb{Z}^d, \mathcal{T})$ is of the form

$$\psi^{\uparrow}(x)(n) = \bigwedge_{k\in\mathbb{Z}^d} e'_{k,n}(x(k)) \tag{5.4}$$

$$\psi^{\downarrow}(x)(k) = \bigvee_{n\in\mathbb{Z}^d} d'_{n,k}(x(n)), \tag{5.5}$$

where $(e'_{k,n}, d'_{n,k})$ is an adjunction on $\mathcal{T}$, for every $n, k \in \mathbb{Z}^d$. Equation (5.4), together with condition $\psi^{\uparrow}\tau^2 = \tau\psi^{\uparrow}$, yields

$$\bigwedge_{k\in\mathbb{Z}^d} e'_{k+2m,n}(x(k)) \;=\; \bigwedge_{k\in\mathbb{Z}^d} e'_{k,n-m}(x(k)).$$

Since this identity holds for every $x \in \mathrm{Fun}(\mathbb{Z}^d, \mathcal{T})$ and $n, m \in \mathbb{Z}^d$, we conclude that

$$e'_{k+2m,n} = e'_{k,n-m}, \quad \forall\, k, n, m \in \mathbb{Z}^d.$$

Similarly, equation (5.5), together with condition $\psi^{\downarrow}\tau = \tau^2\psi^{\downarrow}$, leads to the identity

$$d'_{n+m,k} = d'_{n,k-2m}, \quad \forall\, k, n, m \in \mathbb{Z}^d.$$

Set $e_k = e'_{k,0}$ and $d_k = d'_{0,k}$ and observe that (e_k, d_k) constitutes an adjunction on $\mathcal{T}$. A straightforward manipulation shows that

$$e'_{k,n} = e_{k-2n} \quad \text{and} \quad d'_{n,k} = d_{k-2n},$$

whence we arrive at the identities in (5.2) and (5.3). ∎

5.2. Example. Consider the case when $\mathcal{T} = \overline{\mathbb{R}} = \mathbb{R} \cup \{-\infty, +\infty\}$. An important class of adjunctions (e, d) on $\overline{\mathbb{R}}$ are those of the form

$$d(t) = at + b, \quad e(t) = \frac{t}{a} - b$$

where $a \in \mathbb{R} \setminus \{0\},\ b \in \mathbb{R}$ are constants. We can also choose $b = -\infty$ in which case we arrive at the trivial adjunction $e(t) \equiv +\infty$ and $d(t) \equiv -\infty$.

If we choose the adjunctions in (5.2) and (5.3) to be of this form, we arrive at analysis/synthesis operators

$$\psi^{\uparrow}(x)(n) = \bigwedge_{k\in\mathbb{Z}^d} \Big[\frac{x(k)}{a(k-2n)} - b(k-2n)\Big]$$

$$\psi^{\downarrow}(x)(n) = \bigvee_{k\in\mathbb{Z}^d} \big[a(n-2k)x(k) + b(n-2k)\big].$$

In practice, for all but finitely many values of k, we choose $b(k) = -\infty$; the resulting operators are then of the 'FIR type.' When $a(k) = 1$ for every $k \in \mathbb{Z}^d$, the analysis and synthesis operators are invariant under grayscale shifts as well. ∎

Now that we have found a characterization of analysis and synthesis operators which form adjunctions, we may ask ourselves: for which of these pairs is the pyramid condition 3.3 satisfied? The next proposition answers this question. In the following, we define the *support* A of the analysis/synthesis pair (5.2), (5.3), as being the set of all vectors $k \in \mathbb{Z}^d$ for which the adjunction (e_k, d_k) is non-trivial; i.e., $e_k \not\equiv \top$ and $d_k \not\equiv \bot$, where $\bot, \top$ are the least and greatest element of $\mathcal{T}$, respectively. We introduce the following notation: for $n \in \mathbb{Z}^d$, we define

$$\mathbb{Z}^d[n] = \{k \in \mathbb{Z}^d \mid k - n \in 2\mathbb{Z}^d\}.$$

The sets $\mathbb{Z}^d[n]$ yield a disjoint partition of $\mathbb{Z}^d$ into 2^d parts. For $A \subseteq \mathbb{Z}^d$ and $n \in \mathbb{Z}^d$, we set

$$A[n] = A \cap \mathbb{Z}^d[n],$$

which yields a partition of A comprising at most 2^d nonempty and mutually disjoint subsets.

5.3. Proposition. *Consider the analysis/synthesis pair of Proposition 5.1, and let $A \subseteq \mathbb{Z}^d$ denote its support.*

(a) *Suppose that there exists an $a \in A$ such that:*
  (*i*) $A[a] = \{a\}$.
  (*ii*) d_a *is injective.*
  Then the pyramid condition 3.3 is satisfied.

(b) *Assume that the pyramid condition 3.3 holds along with the following condition:*

$$\bigwedge_{k \in A} e_k\Big(\bigvee_{b \in A[k] \setminus \{k\}} d_b(\top)\Big) \neq \bot \tag{5.6}$$

  Then, there exists an $a \in A$ such that $A[a] = \{a\}$.

PROOF. (a): Assume that conditions (*i*) and (*ii*) hold. We show that $\psi^\downarrow$ is injective. From (5.3) notice that

$$\psi^\downarrow(x)(k) \;=\; \bigvee_{m \in A[k]} d_m(x(\frac{k-m}{2})),$$

for every $k \in \mathbb{Z}^d$. If $x_1 \neq x_2$, then $x_1(n) \neq x_2(n)$ for some $n \in \mathbb{Z}^d$. Let $k = 2n + a$, then $A[k] = A \cap \mathbb{Z}^d[2n + a] = A \cap \mathbb{Z}^d[a] = A[a] = \{a\}$; hence, for $i = 1, 2$:

$$\psi^\downarrow(x_i)(k) = d_a(x_i(n)).$$

Since d_a is assumed to be injective, we find that $\psi^\downarrow(x_1)(k) \neq \psi^\downarrow(x_2)(k)$. Therefore, $\psi^\downarrow$ is injective and the pyramid condition 3.3 is satisfied.

(b): Suppose that the given conditions are satisfied and that, for every $k \in A$, $A[k]$ contains more than one element. We will show that this leads to a contradiction. From (5.3) notice that

$$\psi^\downarrow(x)(k) \;=\; \bigvee_{n \in A'[k]} d_{k-2n}(x(n)),$$

where $A'[k] = \{n \in \mathbb{Z}^d \mid k - 2n \in A\}$. It is easy to see that $a \in A[k]$ if and only if $(k-a)/2 \in A'[k]$. Therefore, for every $k \in A$, $A'[k]$ contains more than one element. We now have that

$$\psi^\downarrow(x)(k) = \begin{cases} \gamma(x)(k), & \text{for } k \notin A \\ \gamma(x)(k) \vee d_k(x(0)), & \text{for } k \in A, \end{cases}$$

where

$$\gamma(x)(k) = \bigvee_{n \in A'[k] \setminus \{0\}} d_{k-2n}(x(n)).$$

Notice that $0 \in A'[k]$ iff $k \in A$. Furthermore, when $k \in A$, $A'[k] \setminus \{0\} \neq \emptyset$ since, for every $k \in A$, $A'[k]$ contains more than one element.

Consider now all signals x such that $x(k) = \top$ for $k \neq 0$. Then

$$\gamma(x)(k) = \bigvee_{n \in A'[k] \setminus \{0\}} d_{k-2n}(\top) = \bigvee_{b \in A[k] \setminus \{k\}} d_b(\top).$$

This expression, which does not depend on x, will be denoted by $\gamma(k)$. Thus

$$\psi^{\downarrow}(x)(k) = \gamma(k) \vee d_k(x(0)), \quad \text{for } k \in A. \tag{5.7}$$

Observe that condition (5.6) can be written as

$$\bigwedge_{k \in A} e_k(\gamma(k)) \neq \bot.$$

Choose

$$x(0) \leq \bigwedge_{k \in A} e_k(\gamma(k)),$$

that is

$$x(0) \leq e_k(\gamma(k)), \quad \text{for every } k \in A.$$

Thus, by the adjunction relation we get

$$d_k(x(0)) \leq \gamma(k). \tag{5.8}$$

From (5.7) and (5.8), and for every signal x satisfying $x(k) = \top$, for $k \neq 0$, we find that

$$\psi^{\downarrow}(x)(k) = \gamma(k) = \bigvee_{b \in A[k] \setminus \{k\}} d_b(\top), \quad \text{for every } k \in A.$$

As this expression is independent of the particular choice of $x(0)$, we conclude that the synthesis operator $\psi^{\downarrow}$ is not injective, which is a contradiction. Therefore, there exists an $a \in A$ such that $A[a]$ contains exactly one element, which will necessarily be a. ∎

Now, observe that d_a is injective if and only if $e_a d_a = \mathsf{id}$. Assume that, for every $a \in A$, the following two conditions are satisfied: $d_a(\top) = \top$ and $A[a]$ contains more than one element. Then, the left hand-side expression in (5.6) equals $\top$ (note that $e_a(\top) = \top$, since e_a is an erosion). Thus (5.6) is satisfied. We arrive at the following corollary.

5.4. Corollary. *Consider the analysis/synthesis pair of Proposition 5.1, and let $A \subseteq \mathbb{Z}^d$ denote its support.*

(a) *Suppose that there exists an $a \in A$ such that:*
   (*i*) $A[a] = \{a\}$.
   (*ii*) $e_a d_a = \mathsf{id}$.
   Then the pyramid condition 3.3 is satisfied.

(b) *Assume that $d_a(\top) = \top$, for every $a \in A$, and that the pyramid condition 3.3 holds. Then, there exists an $a \in A$ such that $A[a] = \{a\}$.*

In the following subsection, we consider a particular subclass of analysis and synthesis operators, given by (5.2), (5.3), with (e_a, d_a) being either the trivial adjunction $(\top, \bot)$ or the adjunction $(\mathsf{id}, \mathsf{id})$.

5.1.2. *Pyramids based on flat adjunctions*

Let $A \subseteq \mathbb{Z}^d$ be given and assume that $(e_k, d_k) = (\mathsf{id}, \mathsf{id})$, for $k \in A$, and $(e_k, d_k) = (\top, \bot)$ elsewhere. In other words, A is the support of $(\psi^\uparrow, \psi^\downarrow)$. Now, (5.2), (5.3) reduce to

$$\psi^\uparrow(x)(n) = \bigwedge_{k \in A} x(2n + k) \tag{5.9}$$

$$\psi^\downarrow(x)(k) = \bigvee_{n \in A[k]} x(\frac{k-n}{2}). \tag{5.10}$$

In mathematical morphology, these two operators are called *flat operators*, since they transform flat signals ($x(k) = t_0$, for k in the domain of x, and $\bot$ outside) into flat signals; see [7, Chapter 11]. Flatness of an operator means in particular that no other gray-values than those present in the signal are created. The resulting pyramids make sense for every gray-value set $\mathcal{T} \subseteq \overline{\mathbb{R}}$ and, in particular, for the binary case $\mathcal{T} = \{0, 1\}$. From Corollary 5.4, notice that, if there exists an $a \in A$ such that $A[a] = \{a\}$, then the pyramid condition 3.3 is satisfied.

Since $(\psi^\uparrow, \psi^\downarrow)$ is an adjunction, the approximation signal $\hat{\psi}(x) = \psi^\downarrow\psi^\uparrow(x)$ satisfies $\hat{\psi}(x) \leq x$ (pointwise inequality) and the error signal $y(n) = x(n) - \hat{\psi}(x)(n)$ is nonnegative. The scheme in (5.9), (5.10) has been proposed earlier by Heijmans and Toet in their paper on morphological sampling (with the roles of dilation and erosion interchanged) [12].

5.5. Example (one-dimensional morphological Haar pyramid). Consider the case when $d = 1$ and $A = \{0, 1\}$. It is easy to show that $A[0] = \{0\}$ and $A[1] = \{1\}$. In particular, this means that the pyramid condition 3.3 is satisfied. We get that

$$\psi^\uparrow(x)(n) = x(2n) \wedge x(2n+1) \tag{5.11}$$

$$\psi^\downarrow(x)(2n) = \psi^\downarrow(x)(2n+1) = x(n). \tag{5.12}$$

The diagram in Figure 5 depicts the calculations associated with these operators. Observe that (5.11) and (5.12) are the (morphological) counterparts of (4.5) and (4.6), respectively. The resulting scheme will be called the *morphological Haar pyramid*.

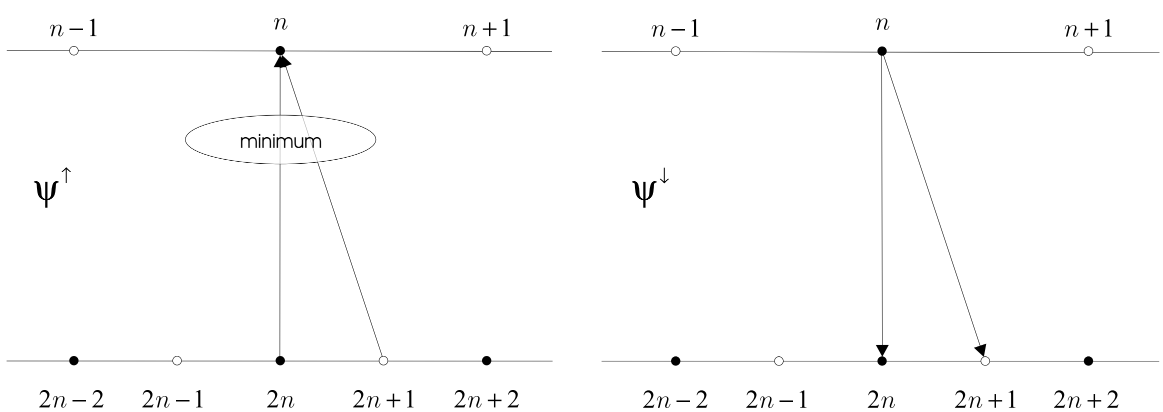

Fig. 5. A diagram illustrating the calculations associated with the analysis and synthesis operators (5.11), (5.12) of a morphological Haar pyramid.

∎

5.6. Example. Another example is obtained by considering the case when $d = 1$ and $A = \{-1, 0, 1\}$. In this case, $A[0] = \{0\}$, $A[1] = A[-1] = \{-1, 1\}$, and the pyramid condition 3.3 is satisfied. We get that

$$\psi^{\uparrow}(x)(n) = x(2n-1) \wedge x(2n) \wedge x(2n+1) \tag{5.13}$$

$$\psi^{\downarrow}(x)(2n) = x(n) \quad \text{and} \quad \psi^{\downarrow}(x)(2n+1) = x(n) \vee x(n+1). \tag{5.14}$$

This leads to a symmetrized version of the morphological Haar pyramid. The diagram in Figure 6 depicts the calculations associated with these operators. ∎

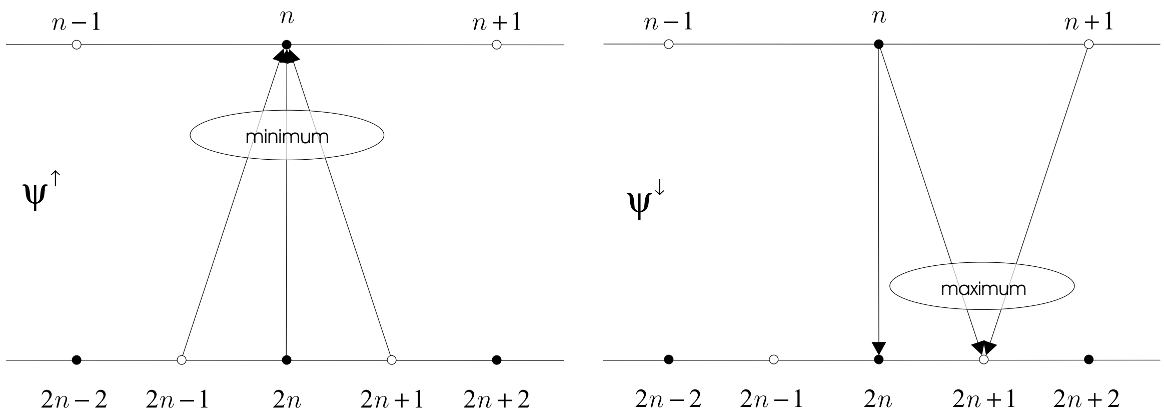

Fig. 6. A diagram illustrating the calculations associated with the analysis and synthesis operators (5.13), (5.14) in Example 5.6.

We now consider a few two-dimensional examples.

5.7. Example (2-dimensional morphological Haar pyramid). Let $A = \{(0,0), (0,1), (1,1), (1,0)\}$. It is evident that $A[m,n] = \{(m,n)\}$ for $(m,n) \in A$. Hence, the pyramid condition 3.3 is again satisfied. The operators $\psi^{\uparrow}$ and $\psi^{\downarrow}$ are now given by

$$\psi^{\uparrow}(x)(m,n) = x(2m,2n) \wedge x(2m,2n+1) \wedge x(2m+1,2n+1) \wedge x(2m+1,2n)$$

$$\psi^{\downarrow}(x)(2m,2n) = \psi^{\downarrow}(x)(2m,2n+1) = \psi^{\downarrow}(x)(2m+1,2n+1) = \psi^{\downarrow}(x)(2m+1,2n) = x(m,n).$$

This is a 2-dimensional extension of the morphological Haar pyramid of Example 5.5. ∎

5.8. Example. A more interesting example is obtained by taking A to be the 3×3 square centered at the origin; i.e., $A = \{(-1,-1), (-1,0), (-1,1), (0,-1), (0,0), (0,1), (1,-1), (1,0), (1,1)\}$. We have $A[0,0] = \{(0,0)\}$, $A[0,\pm 1] = \{(0,-1),(0,1)\}$, $A[\pm 1, 0] = \{(-1,0),(1,0)\}$, and $A[\pm 1, \pm 1] = \{(-1,-1),(-1,1),(1,-1),(1,1)\}$. The operators $\psi^{\uparrow}$ and $\psi^{\downarrow}$ are therefore given by

$$\psi^{\uparrow}(x)(m,n) = \bigwedge_{-1 \le k,l \le 1} x(2m+k, 2n+l), \tag{5.15}$$

and

$$\psi^{\downarrow}(x)(2m,2n) = x(m,n) \tag{5.16}$$

$$\psi^{\downarrow}(x)(2m,2n+1) = x(m,n) \vee x(m,n+1) \tag{5.17}$$

$$\psi^{\downarrow}(x)(2m+1,2n) = x(m,n) \vee x(m+1,n) \tag{5.18}$$

$$\psi^{\downarrow}(x)(2m+1,2n+1) = x(m,n) \vee x(m,n+1) \vee x(m+1,n+1) \vee x(m+1,n). \tag{5.19}$$

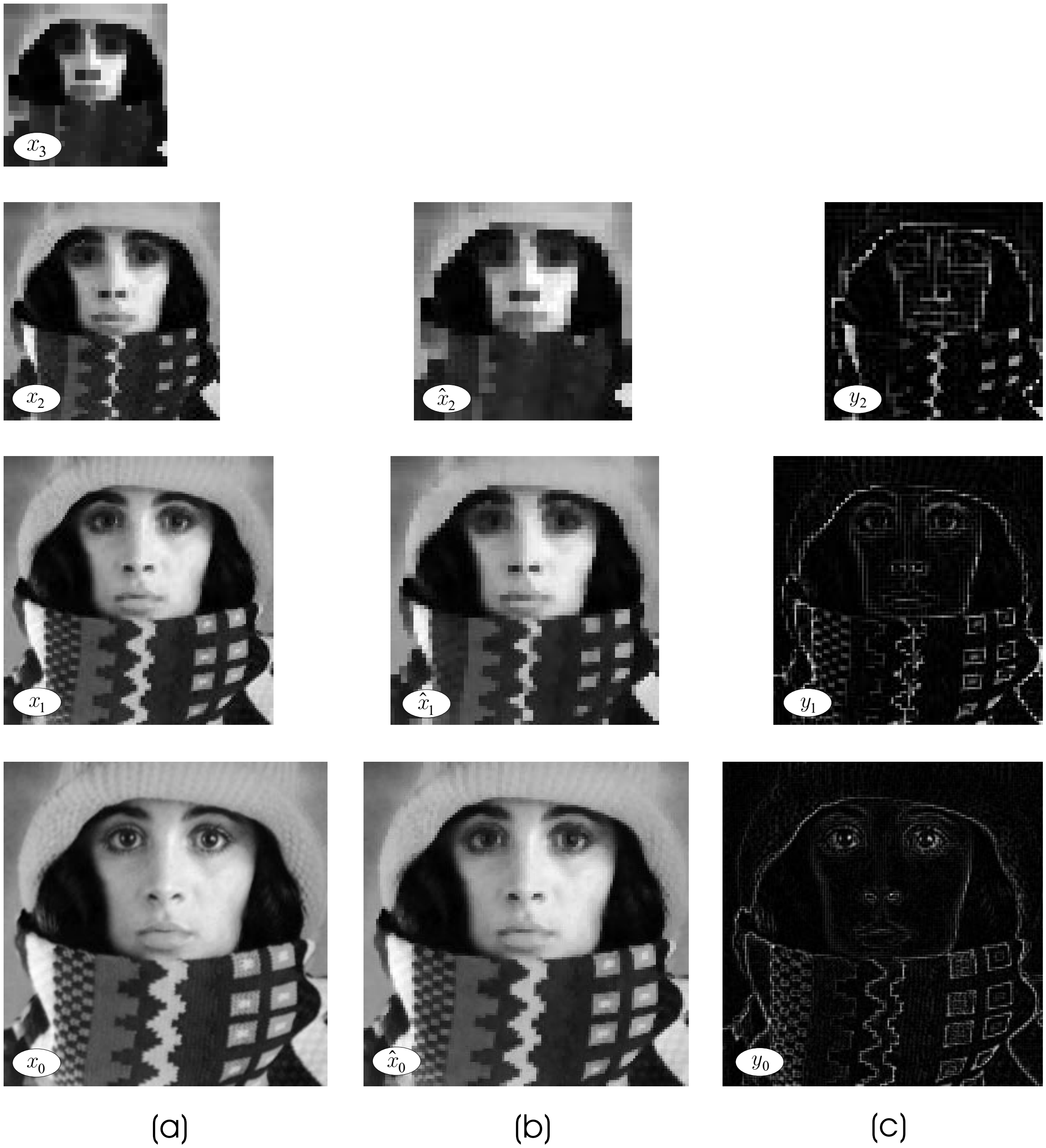

Fig. 7. Multiresolution image decomposition based on the morphological pyramid transform of Example 5.8: (a) An image x_0 and its decomposition $\{x_0, x_1, x_2, x_3\}$ obtained by means of the analysis operator $\psi^{\uparrow}$ in (5.15). (b) The approximation images $\{\hat{x}_0, \hat{x}_1, \hat{x}_2\}$ obtained from $\{x_1, x_2, x_3\}$ by means of the synthesis operator $\psi^{\downarrow}$ in (5.16)–(5.19). (c) The detail images $\{y_0, y_1, y_2\}$.

Clearly, this is a 2-dimensional extension of the pyramid of Example 5.6. An example is depicted in Figure 7.

Operators $\dot{+}$ and $\dot{-}$ are taken here to be the usual addition and difference operators $+$ and $-$. A major difference between the results depicted in Figure 3 and Figure 7 is in the values of the detail signals. The detail signals depicted in Figure 3 assume both positive and negative values, with y_0, y_1, and y_2 taking values in $[-65, 36]$, $[-99, 107]$, and $[-164, 144]$, respectively. On the other hand, the detail signals depicted in Figure 7 assume only nonnegative values. In particular, y_0, y_1, and y_2 take values in $[0, 94]$, $[0, 137]$, and $[0, 145]$, respectively. This can be quite advantageous in image compression and coding applications, as it has been discussed in [13]. ∎

If we take $A = \{0\}$ and $e_0 = d_0 = \mathsf{id}$, then Corollary 5.4 is trivially satisfied. Denoting the corresponding analysis/synthesis pair by $\sigma^{\uparrow}, \sigma_{\perp}^{\downarrow}$ (see Subsection 3.3), we have

$$\sigma^{\uparrow}(x)(n) = x(2n) \tag{5.20}$$
$$\sigma_{\perp}^{\downarrow}(x)(2n) = x(n) \quad \text{and} \quad \sigma_{\perp}^{\downarrow}(x)(m) = \perp, \text{ if } m \notin 2\mathbb{Z}^d.$$

The pair $(\psi^{\uparrow}, \psi^{\downarrow})$ in (5.9), (5.10) can be written as

$$\psi^{\uparrow} = \sigma^{\uparrow}\varepsilon_A \quad \text{and} \quad \psi^{\downarrow} = \delta_A \sigma_{\perp}^{\downarrow}, \tag{5.21}$$

where $(\varepsilon_A, \delta_A)$ is the adjunction given by (2.2), (2.3). This shows that the analysis and synthesis operators of pyramids based on flat adjunctions can be implemented by means of flat erosions, followed by dyadic subsampling by means of $\sigma^{\uparrow}$, and flat dilations, following dyadic upsampling by means of $\sigma_{\perp}^{\downarrow}$.

If we replace the erosion ε_A in (5.21) by the opening $\delta_A \varepsilon_A$, then the pyramid condition is still satisfied, provided that we make an assumption which is stronger than condition (i) in Corollary 5.4. Indeed, we have the following result.

5.9. Proposition. *Let A be a structuring element such that $A[0] = \{0\}$. The analysis operator $\psi^{\uparrow} = \sigma^{\uparrow}\delta_A\varepsilon_A$ and the synthesis operator $\psi^{\downarrow} = \delta_A \sigma_{\perp}^{\downarrow}$ satisfy the pyramid condition.*

PROOF. From the fact that $(\varepsilon_A, \delta_A)$ is an adjunction, we get that

$$\psi^{\uparrow}\psi^{\downarrow} = \sigma^{\uparrow}\delta_A\varepsilon_A\delta_A\sigma_{\perp}^{\downarrow} = \sigma^{\uparrow}\delta_A\sigma_{\perp}^{\downarrow}.$$

Now

$$\begin{aligned}\sigma^{\uparrow}\delta_A\sigma_{\perp}^{\downarrow}(x)(n) &= \bigvee_{k\in A} \sigma_{\perp}^{\downarrow}(x)(2n-k) \\ &= \bigvee_{k\in A[0]} \sigma_{\perp}^{\downarrow}(x)(2n-k) \\ &= \sigma_{\perp}^{\downarrow}(x)(2n) = x(n).\end{aligned}$$

This yields that $\psi^{\uparrow}\psi^{\downarrow} = \mathsf{id}$ and the result is proved. ∎

Notice that the pair $(\psi^{\uparrow}, \psi^{\downarrow})$ in this proposition does not constitute an adjunction. We mention one particular example here.

5.10. Example (Sun–Maragos pyramid). Consider the one-dimensional case, where $V_j = \mathrm{Fun}(\mathbb{Z}, \mathcal{T})$, for every j, and the same analysis and synthesis operators are used at every level j, such that:

$$\psi^{\uparrow}(x)(n) = (x \circ A)(2n) \tag{5.22}$$
$$\psi^{\downarrow}(x)(2n) = x(n) \quad \text{and} \quad \psi^{\downarrow}(x)(2n+1) = x(n) \vee x(n+1). \tag{5.23}$$

Here, $A = \{-1, 0, 1\}$ and $x \circ A = \delta_A\varepsilon_A(x)$, the opening of x by structuring element A. Notice that $A[0] = \{0\}$, as required by Proposition 5.9. The resulting pyramidal decomposition has been suggested by Sun and Maragos in [31] (see also [13]) and is referred to as the *morphological Sun–Maragos pyramid*.

This example can be easily generalized to higher dimensions. Figure 8 depicts the application of the Sun–Maragos pyramid on a binary image. In this case, A is the 3×3 square structuring element, and $\dot{-}$ is the symmetric set difference operator (exclusive OR) of Example 3.5(c). ∎

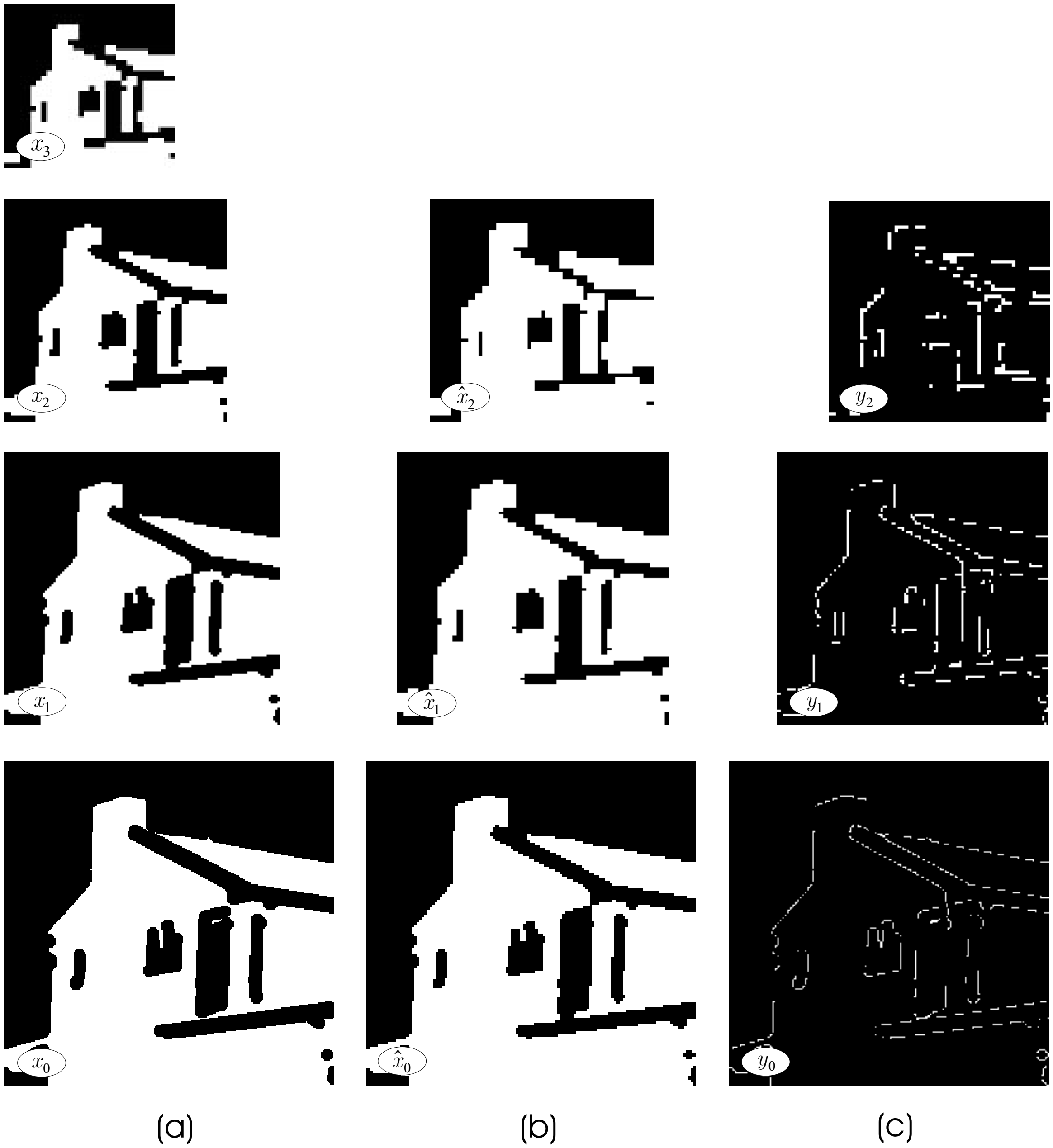

Fig. 8. Multiresolution image decomposition based on the Sun–Maragos pyramid transform: (a) A binary image x_0 and its decomposition $\{x_0, x_1, x_2, x_3\}$ obtained by means of the analysis operator $\psi^{\uparrow}$ in (5.22). (b) The approximation images $\{\hat{x}_0, \hat{x}_1, \hat{x}_2\}$ obtained from $\{x_1, x_2, x_3\}$ by means of the synthesis operator $\psi^{\downarrow}$ in (5.23). (c) The detail images $\{y_0, y_1, y_2\}$.

5.1.3. Non–flat pyramids

The case of non-flat pyramids is similar to that of flat pyramids. Suppose that we replace (5.9) and (5.10) with (see also Example 5.2)

$$\begin{aligned} \psi^{\uparrow}(x)(n) &= \bigwedge_{k\in A} \big[x(2n+k) - b(k)\big] \\ \psi^{\downarrow}(x)(k) &= \bigvee_{n\in A[k]} \big[x(\frac{k-n}{2}) + b(n)\big], \end{aligned}$$

where b is a function with domain A and range in $\mathbb{R}$. In reference to Proposition 5.3, notice that $d_n(t) = t + b(n)$ is injective, for every $n \in \mathbb{Z}^d$. Therefore, if there exists an $a \in A$ such that $A[a] = \{a\}$, then the pyramid condition 3.3 is satisfied.

5.2. Single–scale pyramids

5.2.1. Granulometries

An important tool of mathematical morphology is the so-called *granulometry* [20, 7]. It has been used for several purposes, such as texture classification, shape description, etc. Basically, a granulometry is a family of openings by structuring elements of increasing size. A *discrete* granulometry, on a complete lattice $\mathcal{L}$, is a family of openings $\{\alpha_j \mid j \geq 0\}$ such that

$$\alpha_0 = \mathsf{id} \quad \text{and} \quad \alpha_{j+1} \leq \alpha_j, \quad j \geq 0. \tag{5.24}$$

Notice that (5.24) is equivalent to

$$\alpha_0 = \mathsf{id} \quad \text{and} \quad \alpha_{j+1}\alpha_j = \alpha_{j+1}, \quad j \geq 0.$$

We show here that a given (discrete) granulometry generates its own single-scale pyramid, in terms of adjunctions which satisfy the pyramid condition 3.3.

Suppose we are given a discrete granulometry $\{\alpha_j \mid j \geq 0\}$ on the complete lattice $\mathcal{L}$. Put $V_j = \mathrm{Ran}(\alpha_j)$, that is the range of α_j, and define $\psi_j^\uparrow = \alpha_{j+1}$ and $\psi_j^\downarrow = \mathsf{id}$. It is evident that $\psi_j^\uparrow$ maps V_j into V_{j+1} and $\psi_j^\downarrow$ maps V_{j+1} into V_j, since $V_{j+1} \subseteq V_j$. To show that $(\psi_j^\uparrow, \psi_j^\downarrow)$ defines an adjunction between V_j and V_{j+1} we must show the following relation:

$$y \leq \psi_j^\uparrow(x) \iff \psi_j^\downarrow(y) \leq x, \quad \text{for } x \in \mathrm{Ran}(\alpha_j) \text{ and } y \in \mathrm{Ran}(\alpha_{j+1}).$$

Indeed, writing $x = \alpha_j(x')$ and $y = \alpha_{j+1}(y')$, we find that

$$\begin{aligned} y \leq \psi_j^\uparrow(x) &\iff \alpha_{j+1}(y') \leq \alpha_{j+1}\alpha_j(x') \\ &\iff \alpha_{j+1}(y') \leq \alpha_{j+1}(x') \\ &\iff \alpha_{j+1}(y') \leq \alpha_j(x') \\ &\iff \psi_j^\downarrow(y) \leq x. \end{aligned}$$

In the last but one implication " $\Rightarrow$ " is trivial, since $\alpha_{j+1}(x') \leq \alpha_j(x')$. To get "$\Leftarrow$" observe that $\alpha_{j+1}(y') \leq \alpha_j(x')$ implies that $\alpha_{j+1}(y') = \alpha_{j+1}\alpha_{j+1}(y') \leq \alpha_{j+1}\alpha_j(x') = \alpha_{j+1}(x')$.

The pyramid condition 3.3 holds, since $\psi_j^\uparrow\psi_j^\downarrow = \alpha_{j+1}$ and α_{j+1} coincides with the identity operator on $V_{j+1} = \mathrm{Ran}(\alpha_{j+1})$.

Consider now the case when $\mathcal{L} = \mathrm{Fun}(E, \mathcal{T})$, where $\mathcal{T} \subseteq \overline{\mathbb{R}}$ is a complete lattice. Define

$$\mathcal{T}' = \{t - s \mid t, s \in \mathcal{T} \text{ and } s \leq t\}. \tag{5.25}$$

Take for $\dot{+}$ and $\dot{-}$ the scalar addition and subtraction, respectively. It is evident that the perfect reconstruction condition (3.7) holds. Given an input function $x_0 = x$, we arrive at the signal analysis scheme:

$$\begin{cases} x_0 = x \in V_0 \\ x_{j+1} = \alpha_{j+1}(x_j) \in V_{j+1}, \; j \geq 0 \\ y_j = x_j - x_{j+1}. \end{cases} \tag{5.26}$$

For synthesis, we find that

$$x \;=\; \sum_{j=0}^{\infty} y_j. \qquad (5.27).$$

Given a granulometry $\{\alpha_j \mid j \geq 0\}$ on a complete lattice $\mathcal{L}$, consider the family of negative closings $\beta_j = \alpha_j^*$. It is obvious that

$$\beta_0 = \mathsf{id} \quad \text{and} \quad \beta_{j+1} \geq \beta_j, \quad j \geq 0,$$

and the family $\{\beta_j \mid j \geq 0\}$ is called the (discrete) *anti-granulometry*. We can show that a given (discrete) anti-granulometry generates its own single-scale pyramid as well, in terms of adjunctions which satisfy the pyramid condition 3.3. In the case when $\mathcal{L} = \mathrm{Fun}(E, \mathcal{T})$, this leads to the following signal analysis and synthesis schemes (compare with (5.26), (5.27))

$$\begin{cases} x'_0 = x \in V_0 \\ x'_{j+1} = \beta_{j+1}(x'_j) \in V_{j+1}, \quad j \geq 0 \\ y'_j = x'_{j+1} - x'_j, \end{cases}$$

$$x \;=\; \sum_{j=0}^{\infty} y'_j.$$

In the literature, the decomposition of a signal x into the detail signals $\{..., y'_1, y'_0, y_0, y_1, ...\}$ is called the *discrete size transform* of x [19]. If the space E is finite or countably infinite, then $\{..., |y'_1|, |y'_0|, |y_0|, |y_1|, ...\}$, where $|x| = \sum_{n \in E} |x(n)|$, is called the *pattern spectrum* of x [19].

5.2.2. Morphological skeleton decomposition

We recall Lantuéjoul's formula for discrete skeletons, well-known from mathematical morphology [27]. Let $\mathcal{T} \subseteq \overline{\mathbb{R}}$, define $\mathcal{T}'$ as in (5.25), and consider the set of signals $\mathrm{Fun}(E, \mathcal{T})$. Assume that (ε, δ) is an adjunction on the complete lattice $\mathrm{Fun}(E, \mathcal{T})$. Let $x \in \mathrm{Fun}(E, \mathcal{T})$ and let $K \geq 0$ be such that $\varepsilon^{K+1}(x) = \varepsilon^K(x)$, where $\varepsilon^0 = \mathsf{id}$ and $\varepsilon^j = \varepsilon\varepsilon\cdots\varepsilon$ (j times). Since $\delta\varepsilon$ is an opening, we have that $\varepsilon^j(x) \geq (\delta\varepsilon)\varepsilon^j(x)$. Define $y_j \in \mathrm{Fun}(E, \mathcal{T}')$ by

$$\begin{cases} y_j = \varepsilon^j(x) - (\delta\varepsilon)\varepsilon^j(x), \quad j = 0, 1, \ldots, K-1, \\ y_K = \varepsilon^K(x). \end{cases} \qquad (5.28)$$

It is possible to reconstruct x from $y_0, y_1, \ldots, y_K$ by means of the (backward) recursion formula

$$\begin{cases} x_K = y_K \\ x_j = \delta(x_{j+1}) + y_j, \quad j = K-1, K-2, \ldots, 0. \end{cases}$$

It is easy to verify that $x_j = \varepsilon^j(x)$, hence $x_0 = x$. Figure 9(b) depicts the union of all y_j's in Lantuéjoul's skeleton decomposition of the binary image x depicted in (a), for the case when $\varepsilon(x) = x \ominus A$ and $\delta(x) = x \oplus A$, with A being the 3×3 square structuring element centered at the origin.

Our attempt to fit Lantuéjoul's skeleton decomposition into a pyramid framework is not only successful, but even more, it leads to a decomposition which is better than Lantuéjoul's, in the sense that it contains less data in general.

Assume that $\mathcal{L}$ is a complete lattice and that (ε, δ) is an adjunction on $\mathcal{L}$. Define $V_j = \mathrm{Ran}(\varepsilon^j)$ and let $\psi_j^{\uparrow} : V_j \to V_{j+1}$ and $\psi_j^{\downarrow} : V_{j+1} \to V_j$ be given by

$$\psi_j^{\uparrow} = \varepsilon \quad \text{and} \quad \psi_j^{\downarrow} = \varepsilon^j \delta^{j+1}$$

We can prove the following result.

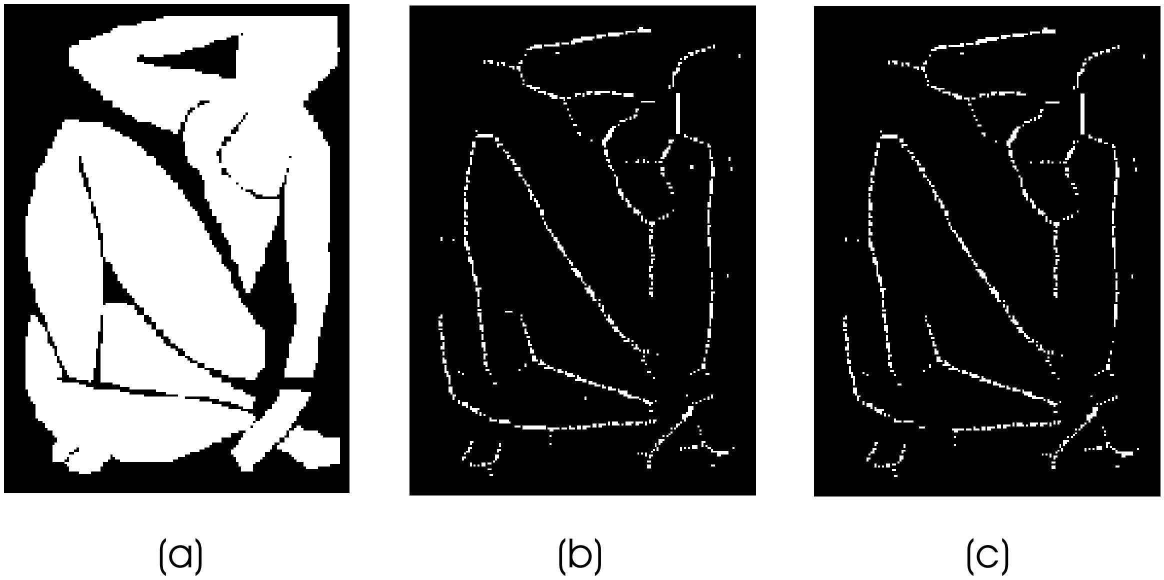

Fig. 9. (a) A binary image, (b) the decomposition obtained by means of Lantuéjoul's skeleton, and (c) the decomposition obtained by means of Goutsias–Schonfeld's skeleton.

5.11. Lemma. *The pair* $(\psi_j^{\uparrow}, \psi_j^{\downarrow})$ *defines an adjunction between* V_j *and* V_{j+1}.

Proof. We must show that $\psi_j^{\downarrow}(y) \le x \iff y \le \psi_j^{\uparrow}(x)$, for $x \in V_j$ and $y \in V_{j+1}$. We write $x = \varepsilon^j(x')$ and $y = \varepsilon^{j+1}(y')$. In the following, we use the fact that, if (ε, δ) is an adjunction, then $(\varepsilon^j, \delta^j)$ is an adjunction as well, for every $j \ge 0$.

'$\Rightarrow$': Assume that $\psi_j^{\downarrow}(y) \le x$; i.e., $\varepsilon^j\delta^{j+1}\varepsilon^{j+1}(y') \le \varepsilon^j(x')$. Applying $\varepsilon^{j+1}\delta^j$ on both sides yields $\varepsilon^{j+1}\delta^j\varepsilon^j\delta^{j+1}\varepsilon^{j+1}(y') \le \varepsilon^{j+1}\delta^j\varepsilon^j(x')$. The left hand-side of this inequality can be written as $\varepsilon(\varepsilon^j\delta^j\varepsilon^j)\delta^{j+1}\varepsilon^{j+1}(y') = \varepsilon\varepsilon^j\delta^{j+1}\varepsilon^{j+1}(y') = \varepsilon^{j+1}\delta^{j+1}\varepsilon^{j+1}(y') = \varepsilon^{j+1}(y') = y$. The right-hand side can be written as $\varepsilon^{j+1}\delta^j\varepsilon^j(x') = \varepsilon(\varepsilon^j\delta^j\varepsilon^j)(x') = \varepsilon\varepsilon^j(x') = \psi_j^{\uparrow}(x)$. Thus, we get $y \le \psi_j^{\uparrow}(x)$.

'$\Leftarrow$': Assume that $y \le \psi_j^{\uparrow}(x)$; i.e., $y \le \varepsilon\varepsilon^j(x') = \varepsilon^{j+1}(x')$. From the fact that $(\varepsilon^{j+1}, \delta^{j+1})$ is an adjunction, we derive that $\delta^{j+1}(y) \le x'$. Applying ε^j on both sides, we get that $\varepsilon^j\delta^{j+1}(y) \le \varepsilon^j(x')$, that is $\psi_j^{\downarrow}(y) \le x$. ∎

It is obvious that $\psi_j^{\uparrow}$ is surjective. We therefore conclude (see Section 5) that the pyramid condition 3.3 holds.

Let us now assume that the underlying lattice $\mathcal{L}$ is of the form $\mathrm{Fun}(E, \mathcal{T})$, where $\mathcal{T} \subseteq \overline{\mathbb{R}}$. We can set $Y_j = \mathrm{Fun}(E, \mathcal{T}')$, where $\mathcal{T}'$ is given by (5.25), and consider $\dot{+}$, $\dot{-}$ to be standard addition and subtraction. Given an input $x_0 = x \in V_0 = \mathrm{Fun}(E, \mathcal{T})$, we arrive at the following signal analysis scheme:

$$\begin{cases} x_0 = x \in V_0 \\ x_{j+1} = \varepsilon(x_j) \in V_{j+1}, \ j \ge 0 \\ y_j = x_j - \varepsilon^j\delta^{j+1}(x_{j+1}). \end{cases} \tag{5.29}$$

For synthesis, we find

$$x = x_0, \quad x_j = \varepsilon^j\delta^{j+1}(x_{j+1}) + y_j, \quad j \ge 0. \tag{5.30}$$

Notice that the detail signal y_j can be written as

$$y_j = \varepsilon^j(x) - (\varepsilon^j\delta^j)(\delta\varepsilon)\varepsilon^j(x). \tag{5.31}$$

Comparing (5.31) to the original Lantuéjoul formula (5.28), we see that in our new decomposition we have an extra closing $\varepsilon^j\delta^j$. As a result, the detail signal y_j in (5.31) is never larger than the detail signal in the Lantuéjoul formula (5.28). It therefore gives rise to a more efficient compression. This skeleton decomposition has been found earlier by Goutsias and Schonfeld [6]. Figure 9(c) depicts the result of applying this decomposition to the binary image in (a). The resulting image is different than the one depicted in Figure 9(b) in 66 pixels. Since the image depicted in Figure 9(b) is non-zero at 1,453 pixels, this amounts to 4.5% data reduction.

An alternative approach to signal decomposition, suggested by Kresch [14], is to set $Y_j = \mathrm{Fun}(E, \mathcal{T})$ and define $\dot{-}$ by means of (3.11). In this case, $\dot{+}$ is given by (3.12). Given an input $x_0 = x \in V_0 = \mathrm{Fun}(E, \mathcal{T})$, we arrive at the following signal analysis scheme:

$$\begin{cases} x_0 = x \in V_0 \\ x_{j+1} = \varepsilon(x_j) \in V_{j+1}, \ j \geq 0 \\ y_j(n) = \begin{cases} x_j(n), \ \text{if } x_j(n) \neq \varepsilon^j\delta^{j+1}(x_{j+1})(n) \\ \bot, \ \text{otherwise} \end{cases} \end{cases}.$$

The synthesis scheme looks as follows:

$$x = x_0, \quad x_j = \varepsilon^j\delta^{j+1}(x_{j+1}) \vee y_j, \quad j \geq 0. \tag{5.32}$$

Notice that the detail signal y_j can be written as

$$y_j(n) = \begin{cases} \varepsilon^j(x)(n), \ \text{if } \varepsilon^j(x)(n) \neq (\varepsilon^j\delta^j)(\delta\varepsilon)\varepsilon^j(x)(n) \\ \bot, \ \text{otherwise} \end{cases}.$$

Assume again that there exists a $K \geq 0$ such that $\varepsilon^{K+1}(x) = \varepsilon^K(x)$ and set $y_K = \varepsilon^K(x)$. Apply δ^j on both sides of (5.32), and use the fact that δ^j distributes over suprema; we find

$$\delta^j(x_j) = \delta^{j+1}(x_{j+1}) \vee \delta^j(y_j).$$

This implies the following formula:

$$\delta^{K-k}(x_{K-k}) = \bigvee_{j=0}^{k} \delta^{K-j}(y_{K-j}), \quad k = 0, 1, \ldots, K.$$

Substitution of $k = K$ yields

$$x_0 = \bigvee_{k=0}^{K} \delta^k(y_k).$$

Thus, the original signal can be recovered as a supremum of dilations of the detail signal.

The Goutsias–Schonfeld and Kresch skeleton decomposition schemes are quite different, even though they satisfy the same algebraic description. Figure 10 depicts the results of applying these decompositions to a grayscale image x. The 3×3 structuring element A that contains the origin has been used in both cases. In the Goutsias–Schonfeld case, y_0 is the top-hat transform of x, since $y_0 = x - x \bigcirc A$. However, the detail signal y_0 in the Kresch case takes value zero (it is black) at all pixels at which $x = x \bigcirc A$ and equals x at all other pixels.

5.12. Remark. We have assumed that the underlying space is a complete lattice, but it is not difficult to show that, as long as we restrict ourselves to finite decompositions, it suffices to assume that $\mathcal{L}$ is a lattice, not necessarily complete. This means that the set $\mathcal{T} \subseteq \overline{\mathbb{R}}$ of gray-values can be arbitrary.

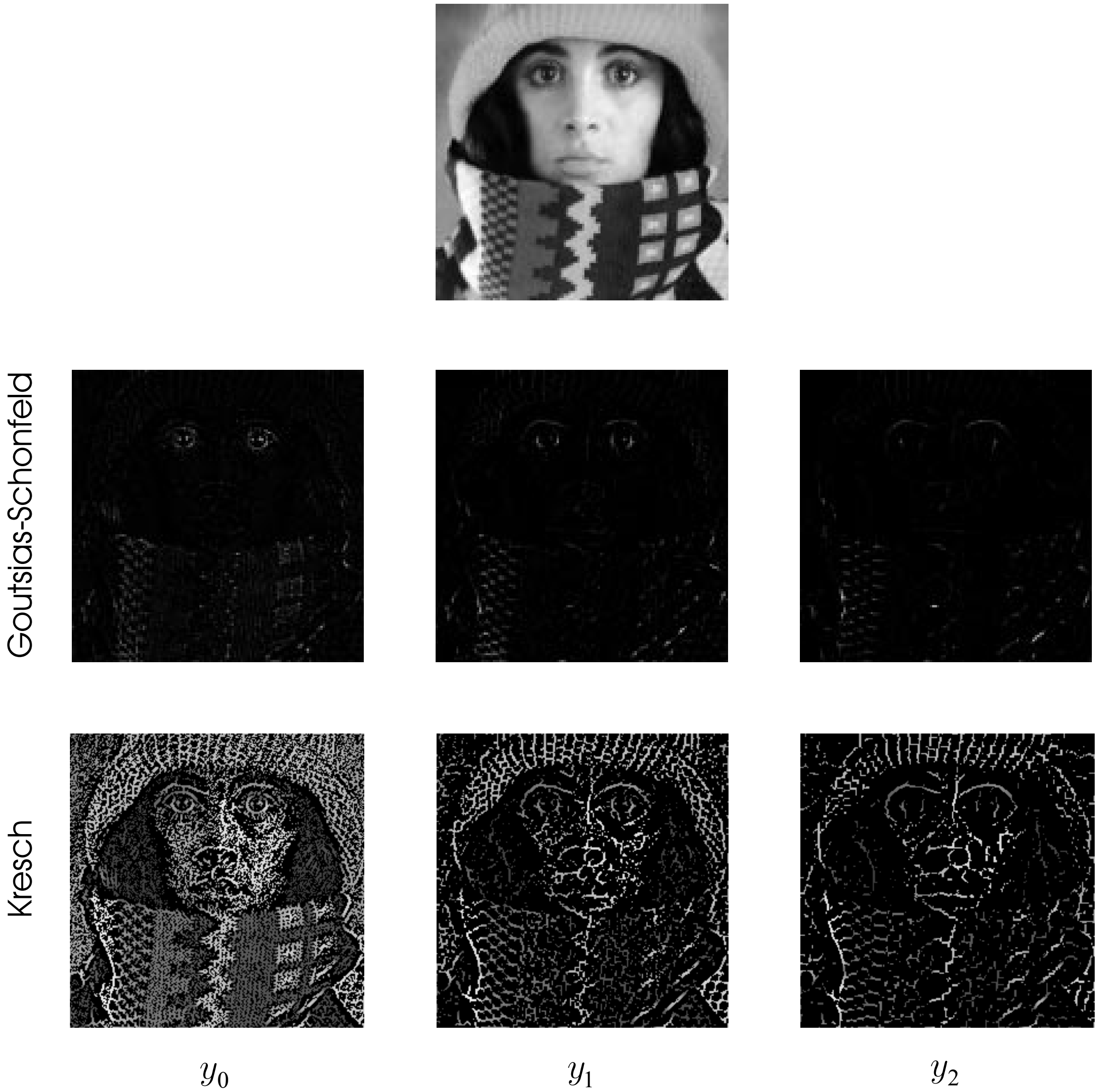

Fig. 10. A grayscale image and the decompositions obtained by means of the Goutsias–Schonfeld and Kresch skeleton transforms.

5.3. A generalization

The construction that led to (5.29), (5.30) can be easily generalized to include adjunction pyramids as well. Indeed, assume that $\mathcal{L}_j$, $j \geq 0$, are complete lattices and that $(\psi_j^\uparrow, \psi_j^\downarrow)$ is an adjunction between $\mathcal{L}_j$ and $\mathcal{L}_{j+1}$. Define $\psi_{0,j}^\uparrow$ and $\psi_{j,0}^\downarrow$ by means of (3.1), (3.2), and let β_j be the closing on $\mathcal{L}_j$ given by

$$\beta_j = \psi_{0,j}^\uparrow \psi_{j,0}^\downarrow,$$

where $\beta_0 = \mathsf{id}$. Let the complete lattices V_j be defined as

$$V_j = \mathrm{Ran}(\beta_j).$$

Observe that $V_0 = \mathcal{L}_0$. The following analogue of Lemma 5.11 holds:

5.13. Lemma. *The pair $(\psi_j^\uparrow, \beta_j \psi_j^\downarrow)$ defines an adjunction between V_j and V_{j+1}.*

Furthermore, it is not difficult to see that $\psi_j^\uparrow$ is surjective. Namely, let $y = \beta_{j+1}(x) \in V_{j+1}$, then $y = \psi_j^\uparrow \psi_{0,j}^\uparrow \psi_{j,0}^\downarrow \psi_j^\downarrow(x) = \psi_j^\uparrow \beta_j \psi_j^\downarrow(x) = \psi_j^\uparrow(x')$, where $x' = \beta_j \psi_j^\downarrow(x) \in V_j$. Therefore, the pyramid condition 3.3 is satisfied in this case.

This generalization can be very useful in cases when pyramids are used for data compression. It simply says that, from any adjunction pyramid, with analysis and synthesis operators $\psi_j^\uparrow$, $\psi_j^\downarrow$, we can construct a new adjunction pyramid, with analysis and synthesis operators $\psi_j^\uparrow$, $\beta_j \psi_j^\downarrow$, where $\beta_j = \psi_{j-1}^\uparrow \psi_{j-2}^\uparrow \cdots \psi_0^\uparrow \psi_0^\downarrow \psi_1^\downarrow \cdots \psi_{j-1}^\downarrow$, such that, if $y_j' = x_j - \beta_j \psi_j^\downarrow \psi_j^\uparrow(x_j)$ is the detail signal of the second pyramid, then $y_j' \leq y_j$, for every $j > 0$, where $y_j = x_j - \psi_j^\downarrow \psi_j^\uparrow(x_j)$ is the detail signal of the first pyramid (however, notice that $y_0' = y_0$). It is therefore expected that the new pyramid will contain less data in general.

6. Other Nonlinear Pyramids

In this section, we first present a number of nonlinear pyramids that are not based on adjunctions. We then discuss the possibility of combining gray-value quantization and sample reduction into one scheme in such a way that the pyramid condition is satisfied.

6.1. Morphological pyramids

To avoid aliasing, sampling is usually preceded by filtering. Here, we discuss a morphological pyramid scheme in which sampling is followed by filtering.

Let $\mathcal{L} = \mathrm{Fun}(\mathbb{Z}^d, \mathcal{T})$, where $\mathcal{T}$ is a complete chain, and consider the elementary sampling scheme given by $\sigma^\uparrow$ and $\sigma_t^\downarrow$ in Subsection 3.3. Here, $t \in \mathcal{T}$ is a fixed element; in practice one chooses $t = \bot$ or $\top$. Given operators $\phi_j : \mathcal{L} \to \mathcal{L}$, we define $V_j = \mathrm{Ran}(\phi_j)$ and

$$\psi_j^\uparrow = \phi_{j+1}\sigma^\uparrow \quad \text{and} \quad \psi_j^\downarrow = \phi_j \sigma_t^\downarrow.$$

The pyramid condition 3.3 can be written as

$$\phi_{j+1}\sigma^\uparrow \phi_j \sigma_t^\downarrow \phi_{j+1} = \phi_{j+1}.$$

When all ϕ_j's are identical, say ϕ, the previous condition can be stated as follows:

$$\phi\sigma^\uparrow \phi \sigma_t^\downarrow \phi = \phi \quad \text{on} \quad \mathcal{L}. \tag{6.1}$$

6.1. Example. Consider the one-dimensional case. Let α be the opening by a structuring element consisting of three points: $\alpha = \alpha_A$, where $A = \{-1, 0, 1\}$. It is easy to verify that $\sigma^\uparrow \alpha \sigma_\top^\downarrow = \mathsf{id}$ on $\mathrm{Fun}(\mathbb{Z}^d, \mathcal{T})$, and this yields that (6.1) holds, for $\phi = \alpha$ and $t = \top$. It is not difficult to extend this example to the higher-dimensional case. ∎

6.2. Example (Toet pyramid). In this (one-dimensional) example, we use the alternating filter $\phi = \beta\alpha$, where α and β are the opening and closing by the structuring element $A = \{0, 1\}$, and choose $t = \top$. To show the validity of (6.1), for $\phi = \beta\alpha$, consider the diagram of Figure 11.

The input signal $x \in V_{j+1}$ has three consecutive values $x(n-1) = r,\ x(n) = s,\ x(n+1) = t$. It is easy to verify that the output value $s' = (\sigma^\uparrow \beta\alpha\sigma_\top^\downarrow)(x)(n)$ is given by $s' = (s \vee t) \wedge (r \vee s)$. Since the input signal x is an element of $\mathrm{Ran}(\beta\alpha)$, it is impossible that $t > s$ and $r > s$. This yields that $s' = s$; hence, the pyramid condition follows.

The resulting pyramidal signal decomposition scheme has been suggested by Toet in [32]. It can be easily extended to the d–dimensional case; there, one chooses $A = \{0, 1\}^d$. ∎

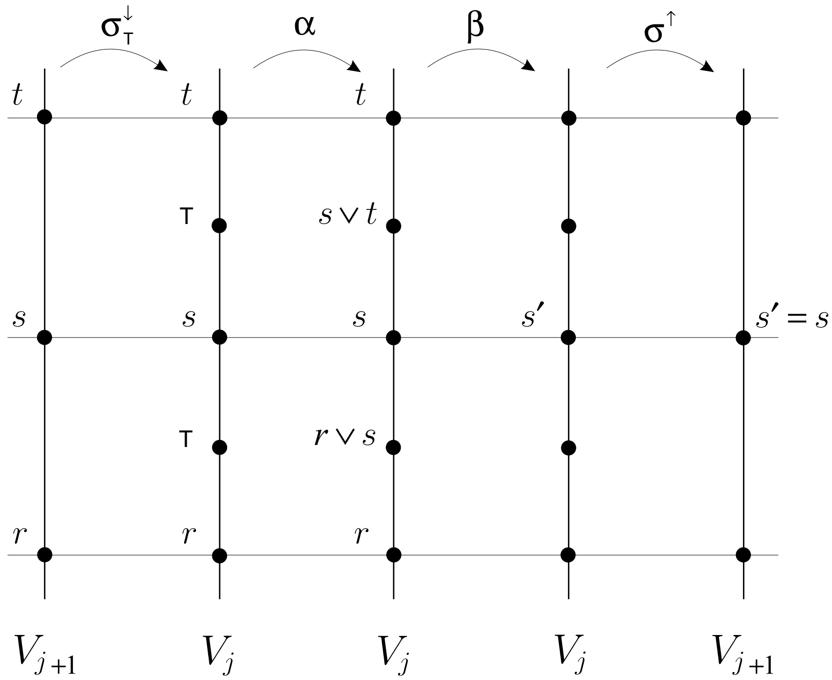

Fig. 11. A diagram illustrating the validity of condition (6.1) for the case when $\phi = \beta\alpha$.

6.2. Median pyramids

It has been suggested in [29] that median filtering can be used to obtain a useful nonlinear pyramid that preserves details and produces a decomposition that can be compressed more efficiently than other (linear) hierarchical signal decomposition schemes. In this example, we show how to build pyramids based on median filtering that satisfy the pyramid condition 3.3.

Assume that $\mathcal{T}$ is a complete chain, and consider a pyramid for which $V_j = \mathrm{Fun}(\mathbb{Z}, \mathcal{T})$, for every j, and the same analysis and synthesis operators are used at every level j, given by

$$\psi^{\uparrow}(x)(n) = \mathsf{median}\{x(2n-1), x(2n), x(2n+1)\} \tag{6.2}$$

$$\psi^{\downarrow}(x)(2n) = \psi^{\downarrow}(x)(2n+1) = x(n). \tag{6.3}$$

Obviously, $\psi^{\uparrow}\psi^{\downarrow}(x)(n) = \mathsf{median}\{\psi^{\downarrow}(x)(2n-1), \psi^{\downarrow}(x)(2n), \psi^{\downarrow}(x)(2n+1)\} = \mathsf{median}\{x(n-1), x(n), x(n)\} = x(n)$, which shows that the pyramid condition holds, for every $x \in \mathrm{Fun}(\mathbb{Z}, \mathcal{T})$. Figure 12 depicts the calculations associated with the analysis and synthesis operators (6.2), (6.3). It is worthwhile noticing that, in this case, the structure of the analysis operator (6.2) is similar to the one in the pyramid scheme of Example 5.6 (see Figure 6), whereas the structure of the synthesis operator (6.3) is similar to the one in the morphological Haar pyramid scheme (see Figure 5).

An alternative median pyramid can be constructed by considering the following analysis and synthesis operators:

$$\psi^{\uparrow}(x)(n) = \begin{cases} x(2n), & \text{if } x(2n-1) \wedge x(2n) \wedge x(2n+1) = x(2n) \\ \mathsf{median}\{x(2n-1), x(2n), x(2n+1)\}, & \text{otherwise} \end{cases} \tag{6.4}$$

$$\psi^{\downarrow}(x)(2n) = x(n), \quad \psi^{\downarrow}(x)(2n+1) = x(n) \vee x(n+1). \tag{6.5}$$

In this case, the synthesis operator is a dilation from V_{j+1} into V_j. The structure of both operators in (6.4) and (6.5) is similar to the ones associated with the pyramid of Example 5.6.

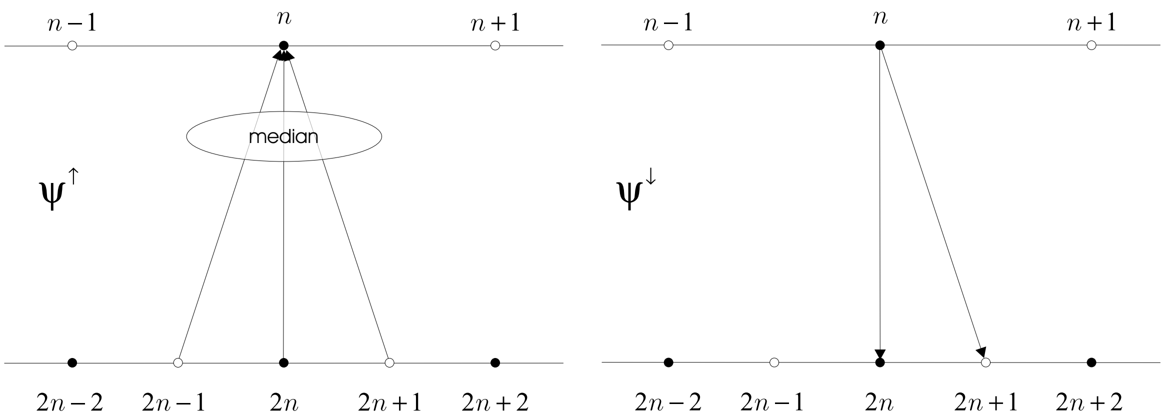

Fig. 12. A diagram illustrating the calculations associated with the analysis and synthesis operators (6.2) and (6.3).

Notice that, if $x(2n-1) \wedge x(2n) \wedge x(2n+1) = x(2n)$, then $\psi^{\uparrow}\psi^{\downarrow}(x)(n) = x(n)$. It can be easily shown that, in all other cases, $\psi^{\uparrow}\psi^{\downarrow}(x)(n) = \mathsf{median}\{\psi^{\downarrow}(x)(2n-1), \psi^{\downarrow}(x)(2n), \psi^{\downarrow}(x)(2n+1)\}$ $= \mathsf{median}\{x(n-1) \vee x(n), x(n), x(n) \vee x(n+1)\} = x(n)$. This shows that the pyramid condition holds, for every $x \in \mathrm{Fun}(\mathbb{Z}, \mathcal{T})$. The median pyramid based on operators (6.4), (6.5) may provide a better approximation $\psi^{\downarrow}\psi^{\uparrow}(x)$ of x than the pyramid based on operators (6.2), (6.3), since the former pyramid utilizes more information from the coarse signal x in order to obtain the sample values $\psi^{\downarrow}(x)(2n+1)$ (compare (6.3) with (6.5)).

The previous pyramids are one-dimensional. We can obtain a 2-dimensional median pyramid, that is the analogue of the morphological pyramid of Example 5.8, by assuming that $V_j = \mathrm{Fun}(\mathbb{Z}^2, \mathcal{T})$, for every j, by using the same analysis and synthesis operators at every level j, and by setting

$$\psi^{\uparrow}(x)(m,n) = \mathsf{median}\{x(2m+k, 2n+l) \mid (k,l) \in A\}, \tag{6.6}$$

where A is the 3×3 square centered at the origin. Take,

$$\psi^{\downarrow}(x)(2m,2n) = x(m,n) \tag{6.7}$$

$$\psi^{\downarrow}(x)(2m,2n+1) = x(m,n) \wedge x(m,n+1) \tag{6.8}$$

$$\psi^{\downarrow}(x)(2m+1,2n) = x(m,n) \wedge x(m+1,n) \tag{6.9}$$

$$\psi^{\downarrow}(x)(2m+1,2n+1) = x(m,n) \vee x(m,n+1) \vee x(m+1,n+1) \vee x(m+1,n). \tag{6.10}$$

It is easy to verify that $\psi^{\uparrow}\psi^{\downarrow} = \mathsf{id}$, which means that the pyramid condition holds. An example, illustrating the resulting 2-dimensional median pyramid is depicted in Figure 13.

6.3. Pyramids with quantization

An issue that we have not touched upon so far is the topic of quantization. Suppose that the gray-values of the signals at the bottom level of a pyramid are represented by at most N bits. In other words, the gray-value set equals $\mathcal{T}_N = \{0, 1, \ldots, 2^N - 1\}$. The operators involved in a pyramid decomposition scheme may map a signal onto one with values outside this range. In particular, this holds for the linear pyramids discussed in Section 4. In such cases, a quantization step, which reduces the transformed gray-value set, may be indispensable. Also, in cases where the gray-value set does not change by the analysis and synthesis operators (e.g., in the case of

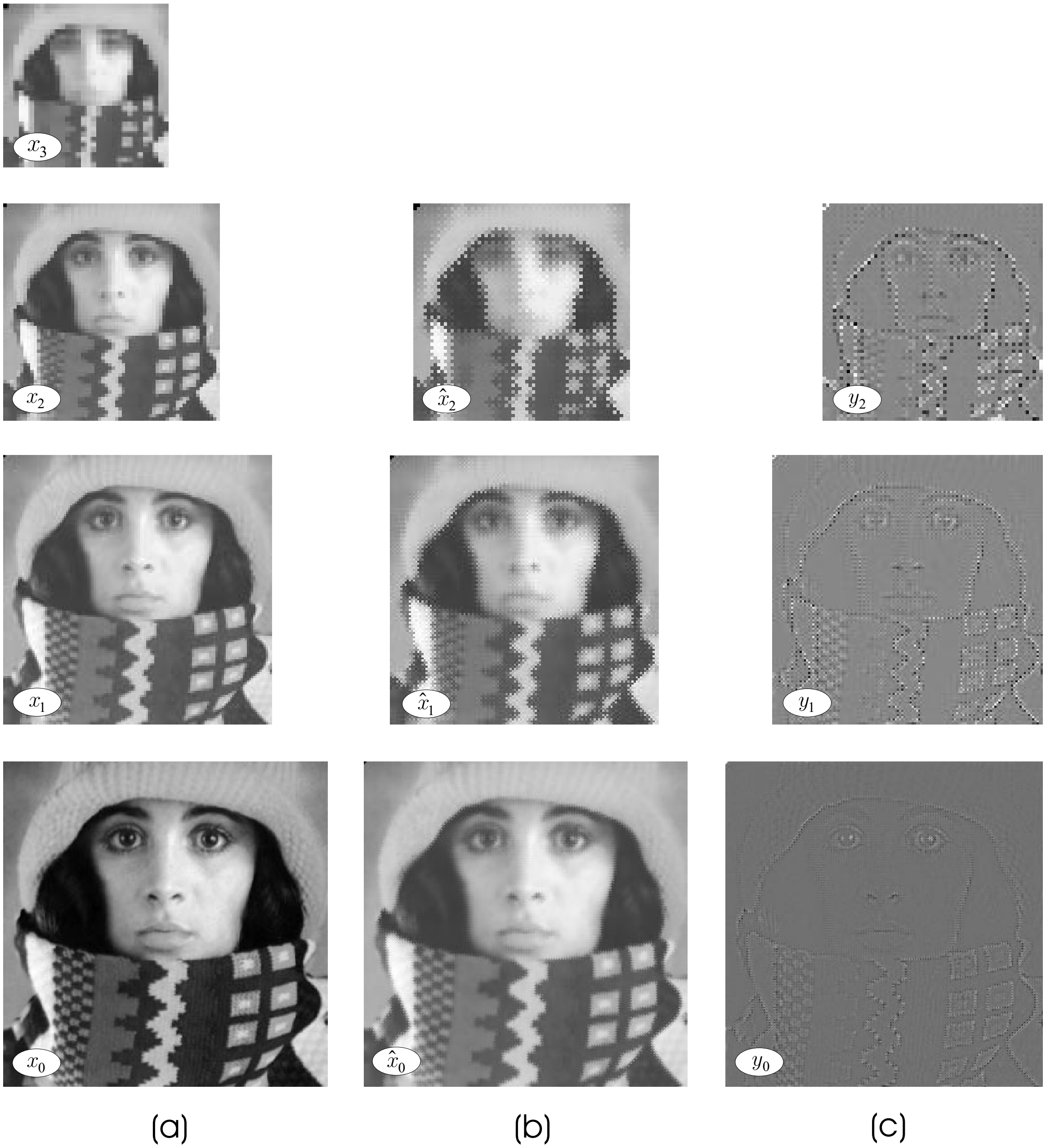

Fig. 13. Multiresolution image decomposition based on a median pyramid: (a) An image x_0 and its decomposition $\{x_0, x_1, x_2, x_3\}$ obtained by means of the analysis operator $\psi^{\uparrow}$ in (6.6). (b) The approximation images $\{\hat{x}_0, \hat{x}_1, \hat{x}_2\}$ obtained from $\{x_1, x_2, x_3\}$ by means of the synthesis operator $\psi^{\downarrow}$ in (6.7)–(6.10). (c) The detail images $\{y_0, y_1, y_2\}$.

flat morphological operators), quantization may be useful in data compression (see Example 6.3 below). In this subsection, we briefly discuss the problem of quantization in the context of morphological operators.

Consider the quantization mapping $q : \mathcal{T}_N \to \mathcal{T}_{N-1}$, given by

$$q(t) = \lfloor t/2 \rfloor,$$

where $\lfloor \cdot \rfloor$ denotes the floor function. For simplicity, we use the same symbol to denote quantization on function spaces; i.e., q can also be considered as the operator from $\mathrm{Fun}(E, \mathcal{T}_N)$ to

$\mathrm{Fun}(E, \mathcal{T}_{N-1})$, given by

$$q(x)(n) = q(x(n)).$$

There are two different ways of "expanding" a quantized value $t \in \mathcal{T}_{N-1}$ to the original gray-value set $\mathcal{T}_N$, namely by means of mappings

$$d(t) = 2t \quad \text{or} \quad e(t) = 2t + 1.$$

Again, we use the same notation for their extensions to the corresponding function spaces. The following properties hold:

$$\begin{aligned} qd(t) = qe(t) = t, &\quad t \in \mathcal{T}_{N-1} \\ dq(t) \le t \le eq(t), &\quad t \in \mathcal{T}_N. \end{aligned} \tag{6.11}$$

Furthermore, q, d, and e are increasing mappings. It immediately follows that (e, q) is an adjunction from $\mathcal{T}_{N-1}$ to $\mathcal{T}_N$ and that (q, d) is an adjunction from $\mathcal{T}_N$ to $\mathcal{T}_{N-1}$. In what follows, we only use the second adjunction. Similar results can be obtained by using the first one as well.

If we want to emphasize the dependence of q and d on N, we write q_N and d_N. It is obvious how the corresponding operators can be used to construct a single-scale pyramid: remove one bit of information at every analysis step. We can formalize this in the following way: put $V_j = \mathrm{Fun}(E, \mathcal{T}_{N-j})$ and define

$$\psi_j^\uparrow = q_{N-j} \quad \text{and} \quad \psi_j^\downarrow = d_{N-j}.$$

Notice that (6.11) guarantees that the pyramid condition 3.3 is satisfied. The following example shows that is possible to combine quantization and (morphological) sample reduction into one scheme in such a way that the pyramid condition 3.3 remains satisfied.

6.3. Example (Morphological pyramid with quantization). Consider the flat adjunction pyramid, given by (5.9), (5.10), where $V_j = \mathrm{Fun}(\mathbb{Z}^d, \mathcal{T}_N)$, in which case

$$\begin{aligned} \psi^\uparrow(x)(n) &= \bigwedge_{k \in A} x(2n + k) \\ \psi^\downarrow(x)(k) &= \bigvee_{n \in A[k]} x(\frac{k - n}{2}). \end{aligned}$$

Assume that, for some $a \in A$, $A[a] = \{a\}$; this yields that the pyramid condition 3.3 is satisfied. Put $\overline{V}_j = \mathrm{Fun}(\mathbb{Z}^d, \mathcal{T}_{N-j})$ and define quantized analysis and synthesis operators between $\overline{V}_j$ and $\overline{V}_{j+1}$ as follows:

$$\begin{aligned} \overline{\psi}_j^\uparrow(x)(n) &= \Big\lfloor \big(\bigwedge_{k \in A} x(2n + k)\big)/2 \Big\rfloor \\ \overline{\psi}_j^\downarrow(x)(k) &= 2\Big(\bigvee_{n \in A[k]} x(\frac{k - n}{2})\Big). \end{aligned}$$

We can write

$$\overline{\psi}_j^\uparrow = q_{N-j}\psi_j^\uparrow \quad \text{and} \quad \overline{\psi}_j^\downarrow = \psi_j^\downarrow d_{N-j}.$$

The pair $(\overline{\psi}_j^\uparrow, \overline{\psi}_j^\downarrow)$ defines an adjunction between $\overline{V}_j$ and $\overline{V}_{j+1}$. Furthermore, the pyramid condition 3.3 is satisfied, since

$$\overline{\psi}_j^\uparrow \overline{\psi}_j^\downarrow = q_{N-j}\psi_j^\uparrow \psi_j^\downarrow d_{N-j} = q_{N-j} d_{N-j} = \mathsf{id} \quad \text{on} \quad \mathrm{Fun}(\mathbb{Z}^d, \mathcal{T}_{N-j-1}).$$

(a) (b)

Fig. 14. (a) A 512×512 grayscale image, and (b) its partial reconstruction obtained from the detail signals $\{y_1, y_2, ..., y_8\}$ calculated by means of the morphological pyramid transform with quantization discussed in Example 6.3.

By taking $\psi^{\uparrow}$ and $\psi^{\downarrow}$ as in (5.15)–(5.19), we can construct a morphological pyramid, like the one in Example 5.8, with the addition of a quantization step at each level.

When the pyramid transform is used for signal compression, the detail signal y_0 is usually removed from the decomposition (this is due to the overcompleteness of the pyramid transform; e.g., see [13]). In this case, satisfactory compression performance can be achieved at the expense of partially reconstructing the original signal x_0. In fact, given the pyramid decomposition $\{y_1, y_2, ..., y_K\}$ of x_0, the inverse pyramid transform reconstructs only an approximation $\hat{x}_0$ of x_0. Figure 14(b) depicts the partial reconstruction of the 512×512 grayscale image depicted in Figure 14(a), obtained by means of inverting the decomposition $\{y_1, y_2, ..., y_8\}$ based on the previously discussed morphological pyramid transform with quantization. Figure 15(b) depicts the number of pixels in $\{y_1, y_2, ..., y_8\}$ as a function of the minimum number of bits required for coding their gray-values (for example, one bit is used to code gray-values 0 and 1, two bits are used to code gray-values 2 and 3, etc.). Figure 15(a) depicts the same graph but for the case of no quantization. In the first case, the graph is skewed towards smaller bit values. This indicates that appropriate coding may produce better compression results when quantization is employed than in the case of no quantization. ∎

7. Multiscale Morphological Operators

The discussion in Subsection 5.1 leads to a new class of nonlinear image processing and analysis tools. These tools are implemented by means of multiscale morphological operators, similar to traditional ones (e.g., erosions, openings, alternating filters, etc.), with one main difference: multiscale operators are implemented by signal subsampling and/or upsampling. In this section, we provide a representative list of basic multiscale morphological operators.

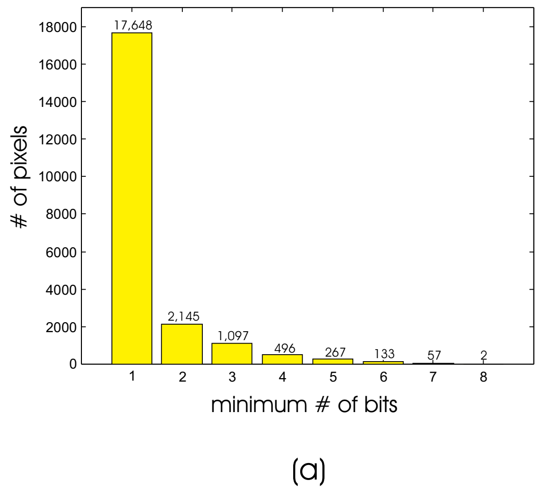

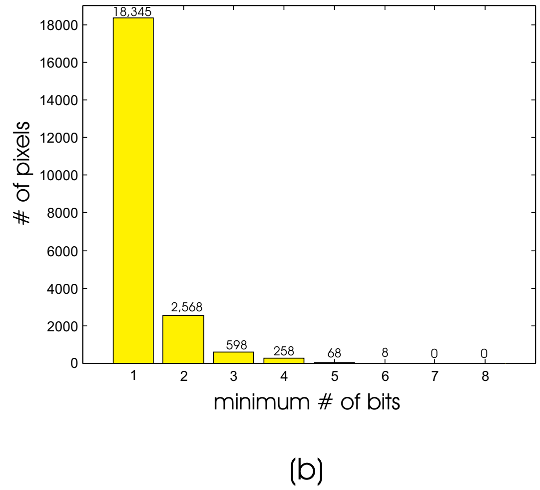

Fig. 15. Number of pixels in $\{y_1, y_2, ..., y_8\}$ of the image depicted in Figure 14(a) as a function of the minimum number of bits required for coding their gray-values, for the case of: (a) the morphological pyramid decomposition discussed in Example 5.8 (without quantization), and (b) the morphological pyramid decomposition with quantization discussed in Example 6.3.

7.1. Erosions and dilations

These are the analysis and synthesis operators of a morphological pyramid based on adjunctions. Of particular interest are flat erosions and dilations, which are simply the operators

$$\epsilon_A^{\uparrow} = \sigma^{\uparrow}\epsilon_A \quad \text{and} \quad \delta_A^{\downarrow} = \delta_A\sigma_{\perp}^{\downarrow}$$

in (5.21), where (ϵ_A, δ_A) is the adjunction given by (2.2), (2.3), and $\sigma^{\uparrow}$, $\sigma_{\perp}^{\downarrow}$ are the (dyadic) subsampling and upsampling operators in Subsection 3.3. As we said before, $(\epsilon_A^{\uparrow}, \delta_A^{\downarrow})$ is an adjunction and $\epsilon_A^{\uparrow}\delta_A^{\downarrow} = \mathsf{id}$, provided that there exists an $a \in A$ such that $A[a] = \{a\}$. If we take A to be the 3×3 square structuring element containing the origin, then this condition is satisfied.

We may consider a two-level morphological pyramid and assume that the pair $(\psi^{\downarrow}, \psi^{\uparrow})$ is an adjunction (instead of $(\psi^{\uparrow}, \psi^{\downarrow})$, as we did in § 5.1.1) between V_0 and V_1. In this case, $\psi^{\uparrow}$ is a dilation and $\psi^{\downarrow}$ is an erosion. This leads to a flat multiscale erosion and dilation of the form

$$\epsilon_A^{\downarrow} = \epsilon_A\sigma_{\top}^{\downarrow} \quad \text{and} \quad \delta_A^{\uparrow} = \sigma^{\uparrow}\delta_A,$$

respectively. The pair $(\epsilon_A^{\downarrow}, \delta_A^{\uparrow})$ is an adjunction and $\delta_A^{\uparrow}\epsilon_A^{\downarrow} = \mathsf{id}$. Notice that $\epsilon_A^{\uparrow}$ and $\delta_{\check{A}}^{\uparrow}$ (where $\check{A} = -A$) are *dual* operators, in the sense that, if $x \in \mathrm{Fun}(\mathbb{Z}^d, \overline{\mathbb{R}})$, then $(\delta_{\check{A}}^{\uparrow}(x))^* = \epsilon_A^{\uparrow}(x^*)$, where $x^*(n) = -x(n)$, for every $n \in \mathbb{Z}^d$. This is a direct consequence of the duality between ϵ_A and $\delta_{\check{A}}$. The same is true for the pair $(\epsilon_A^{\downarrow}, \delta_{\check{A}}^{\downarrow})$. Notice finally that all these operators are translation invariant, in the sense of (5.1). A binary and grayscale example, illustrating flat multiscale erosions and dilations, is depicted in Figure 16; here A is the 3×3 square structuring element.

7.2. Openings and closings

Multiscale openings and closings can be obtained by concatenating the analysis and synthesis operators of a morphological pyramid based on adjunctions. For example, if $(\psi^{\uparrow}, \psi^{\downarrow})$ form an

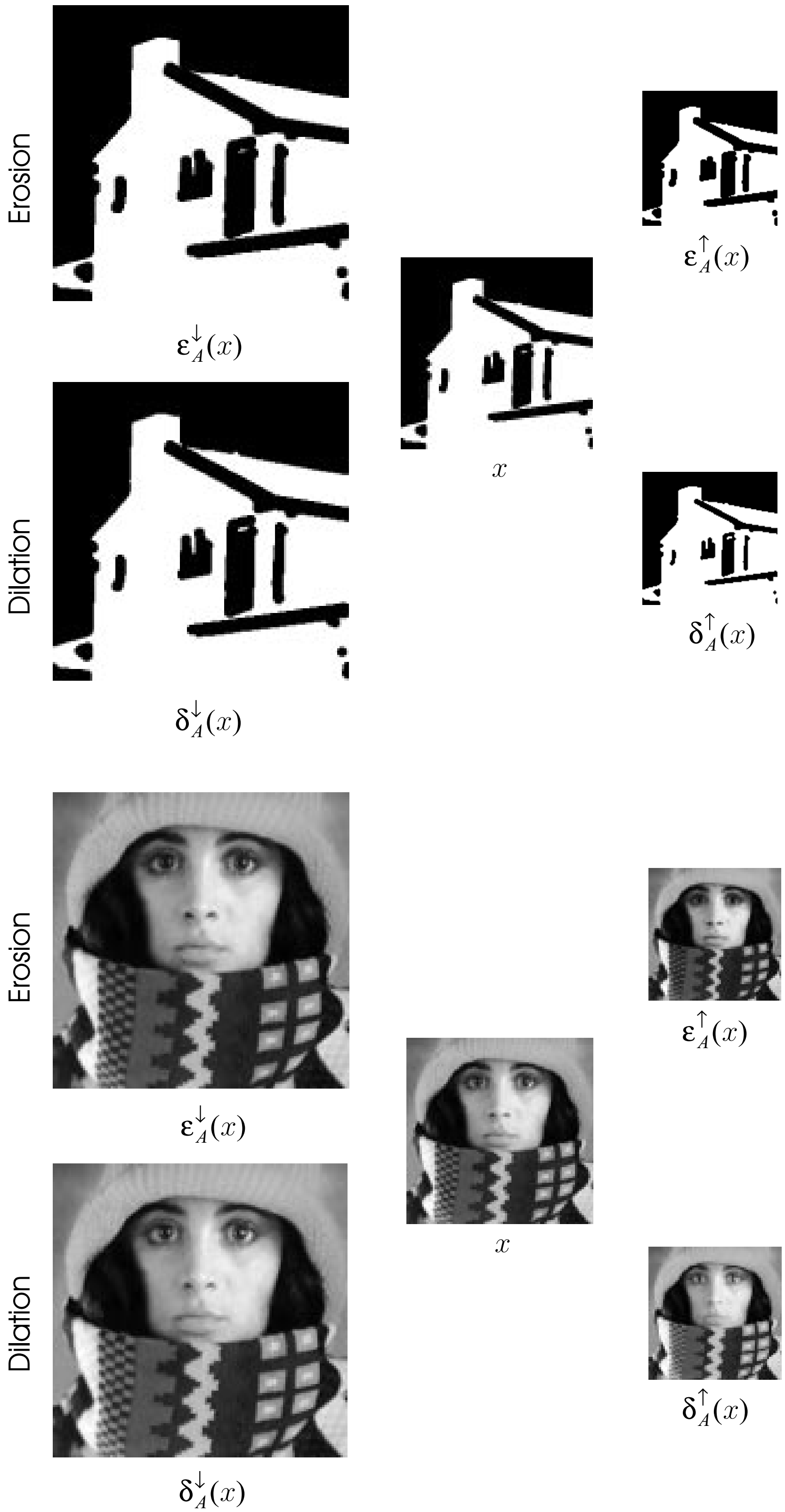

Fig. 16. A binary and grayscale example illustrating the flat multiscale erosions $\epsilon_A^{\uparrow}$, $\epsilon_A^{\downarrow}$ and dilations $\delta_A^{\uparrow}$, $\delta_A^{\downarrow}$, where A is the 3×3 square structuring element.

adjunction, then $\psi^{\downarrow}\psi^{\uparrow}$ is an opening and $\psi^{\uparrow}\psi^{\downarrow}$ is a closing (although a trivial one, if the pyramid condition is satisfied). On the other hand, if $(\psi^{\downarrow}, \psi^{\uparrow})$ is an adjunction, then $\psi^{\downarrow}\psi^{\uparrow}$ is a closing and $\psi^{\uparrow}\psi^{\downarrow}$ an opening (the trivial one, if the pyramid condition is satisfied).

A flat multiscale opening $\alpha_A^{(1)}$ can be obtained by applying erosion $\epsilon_A^{\uparrow}$ followed by dilation $\delta_A^{\downarrow}$; i.e,

$$\alpha_A^{(1)} = \delta_A^{\downarrow}\epsilon_A^{\uparrow} = \delta_A\sigma_{\perp}^{\downarrow}\sigma^{\uparrow}\epsilon_A. \tag{7.1}$$

Notice that $\epsilon_A^{\uparrow}\delta_A^{\downarrow}$ is a trivial closing, since $\epsilon_A^{\uparrow}\delta_A^{\downarrow} = \mathsf{id}$. However, we can build a closing operator $\beta_A^{(1)}$ by means of the adjunction $(\epsilon_A^{\downarrow}, \delta_A^{\uparrow})$, in which case

$$\beta_A^{(1)} = \epsilon_A^{\downarrow}\delta_A^{\uparrow} = \epsilon_A\sigma_{\perp}^{\downarrow}\sigma^{\uparrow}\delta_A. \tag{7.2}$$

$\alpha_A^{(1)}$ and $\beta_A^{(1)}$ are negative operators, since $(\alpha_A^{(1)}(x))^* = \beta_A^{(1)}(x^*)$, and translation invariant, in the sense of (2.1).

Operators (7.1), (7.2) can be extended, by considering a k-level pyramid. Indeed, if we set

$$\alpha_A^{(k)} = \underbrace{\delta_A^{\downarrow}\delta_A^{\downarrow}\cdots\delta_A^{\downarrow}}_{k-\text{times}}\overbrace{\epsilon_A^{\uparrow}\epsilon_A^{\uparrow}\cdots\epsilon_A^{\uparrow}}^{k-\text{times}} \quad \text{and} \quad \beta_A^{(k)} = \underbrace{\epsilon_A^{\downarrow}\epsilon_A^{\downarrow}\cdots\epsilon_A^{\downarrow}}_{k-\text{times}}\overbrace{\delta_A^{\uparrow}\delta_A^{\uparrow}\cdots\delta_A^{\uparrow}}^{k-\text{times}}, \tag{7.3}$$

then it is not difficult to show that $\alpha_A^{(k)}$ is an opening and $\beta_A^{(k)}$ is a closing. We point out that for these observations to hold, the pyramid conditions are not required.

In the binary case, the opening $\alpha_A^{(k)}$ is a multiscale *filter* (i.e., an operator that is increasing and idempotent) that eliminates all pixels in an image x which do not lie inside a replica of the structuring element $(2^k - 1)A$ (where $kA = A \oplus A \oplus \cdots \oplus A$, k-times) translated at a point $(2^k m, 2^k n)$ of $\mathbb{Z}^2$. An analogous argument can be made for the grayscale case as well. A binary and grayscale example, illustrating flat multiscale openings and closings, is depicted in Figure 17.

7.3. Top–hat

Since every opening $\alpha_A^{(k)}(x)$ lies below the signal x itself, the difference $x - \alpha_A^{(k)}(x)$ is nonnegative. This difference contains the residue of approximating x by means of $\alpha_A^{(k)}(x)$. In mathematical morphology, the operator $x - \alpha_A(x)$ is known as the (opening) *top-hat* operator [7]. Therefore, $x - \alpha_A^{(k)}(x)$ is a multiscale (opening) top-hat operator. Notice that, in our terminology, $x - \alpha_A^{(1)}(x)$ is the detail signal obtained at the lowest level of a multiscale adjunction pyramid. Similarly, $\beta_A^{(k)}(x) - x$ is the multiscale closing top-hat operator. A grayscale example, illustrating the single-scale and multiscale top-hat operator, is depicted in Figure 18.

7.4. Morphological filters

In mathematical morphology, any operator that is increasing and idempotent is called a morphological filter. The openings and closings in (2.6), (2.7) are simple examples of morphological filters. By combining them in an appropriate fashion, we form more complicated filters. For example

$$\eta_A = \beta_A\alpha_A \quad \text{and} \quad \xi_A = \alpha_A\beta_A,$$

are morphological filters known as *alternating filters*, whereas

$$\eta_{kA}\eta_{(k-1)A}\cdots\eta_A \quad \text{and} \quad \xi_{kA}\xi_{(k-1)A}\cdots\xi_A,$$

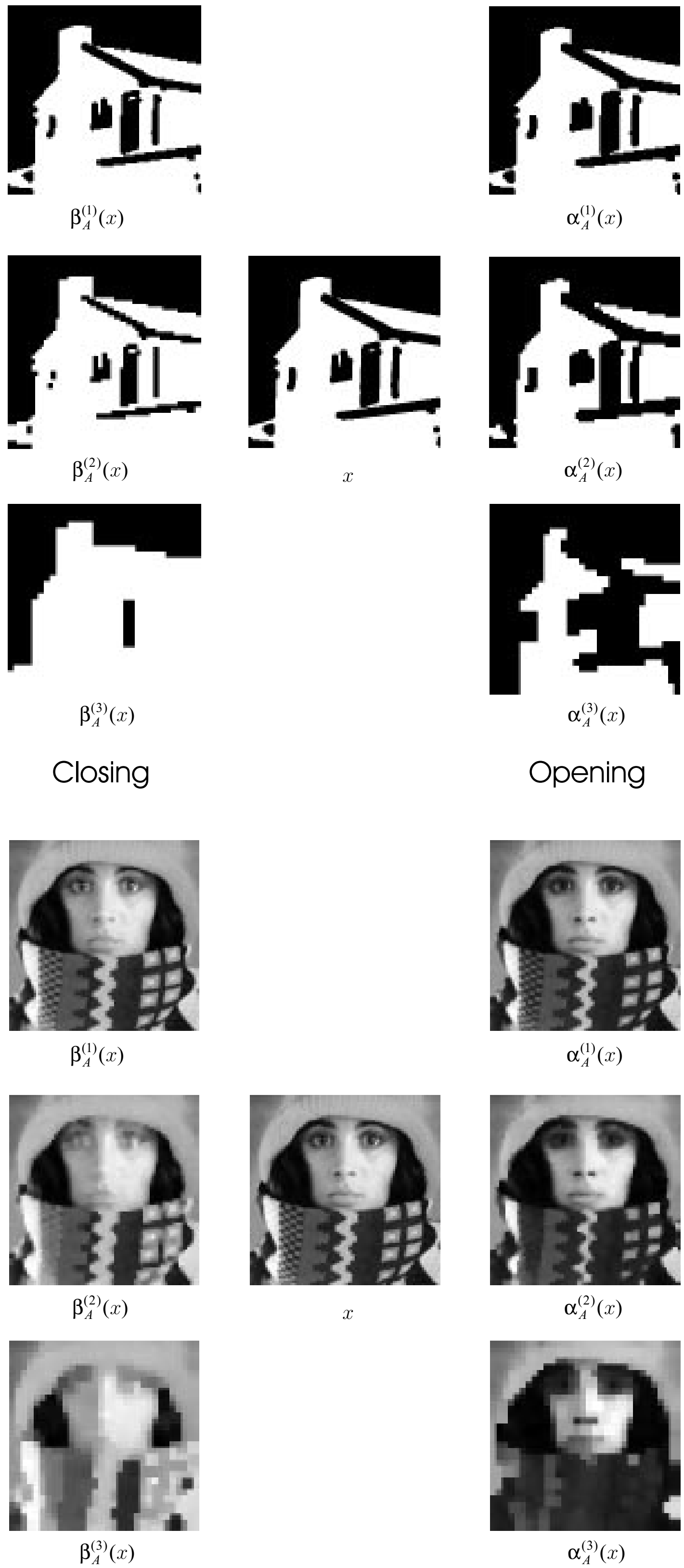

Fig. 17. A binary and grayscale example illustrating the flat multiscale openings $\alpha_A^{(k)}$ and closings $\beta_A^{(k)}$, for $k = 1, 2, 3$, where A is the 3×3 square structuring element.

Fig. 18. A grayscale example illustrating the single-scale and multiscale opening top-hat operators.

where $kA = A \oplus A \oplus \cdots \oplus A$ (k-times), are known as *alternating sequential filters.* Multiscale versions of such operators can be obtained by means of multiscale openings and closings:

$$\eta_A^{(k)} = \beta_A^{(k)} \alpha_A^{(k)} \quad \text{and} \quad \xi_A^{(k)} = \alpha_A^{(k)} \beta_A^{(k)}$$

are multiscale alternating filters and

$$\eta_A^{(k)} \eta_A^{(k-1)} \cdots \eta_A^{(1)} \quad \text{and} \quad \xi_A^{(k)} \xi_A^{(k-1)} \cdots \xi_A^{(1)}$$

are multiscale alternating sequential filters.

Simpler multiscale morphological filters can be obtained by appropriately combining single-scale openings and closings with multiscale erosions and dilations. For example, it can be shown that, for every structuring element B, the operators

$$\delta_A^{\downarrow} \beta_B \epsilon_A^{\uparrow} \quad \text{and} \quad \epsilon_{\check{A}}^{\downarrow} \alpha_{\check{B}} \delta_{\check{A}}^{\uparrow}$$

are *dual* morphological filters. This is a direct consequence of the two pyramid conditions $\epsilon_A^{\uparrow} \delta_A^{\downarrow} = \mathsf{id}$ and $\delta_A^{\uparrow} \epsilon_A^{\downarrow} = \mathsf{id}$. Notice that $\delta_A^{\downarrow} \beta_B \epsilon_A^{\uparrow} \geq \alpha_A^{(1)}$ and $\epsilon_A^{\downarrow} \alpha_B \delta_A^{\uparrow} \leq \beta_A^{(1)}$; refer to [8] for a general account.

Morphological filters are used for noise removal. Figure 19 illustrates the application of a number of single-scale and multiscale morphological filters for recovering a grayscale image x from a noisy version x', corrupted by salt–and–pepper noise. In the single-scale case, the alternating sequential filter $\eta_{2A}\eta_A$ produces the best result. A similar result is however produced by the multiscale filter $\delta_A^{\downarrow} \beta_{2A} \epsilon_A^{\uparrow}$. An important difference between these two filters is implementation speed: implementation of the single-scale alternating sequential filter $\eta_{2A}\eta_A$ requires about four times more operations than for the multiscale filter $\delta_A^{\downarrow} \beta_{2A} \epsilon_A^{\uparrow}$.

These very simple experiments indicate that exploitation of multiscale morphological operators for image filtering is a promising area of research. However, since this topic falls outside the scope of this report, we do not pursue this matter any further here.

7.5. Granulometries

We now show that granulometries (discussed in § 5.2.1), and the associated anti-granulometries, can be easily extended to a multiscale framework by means of pyramid schemes based on adjunctions.

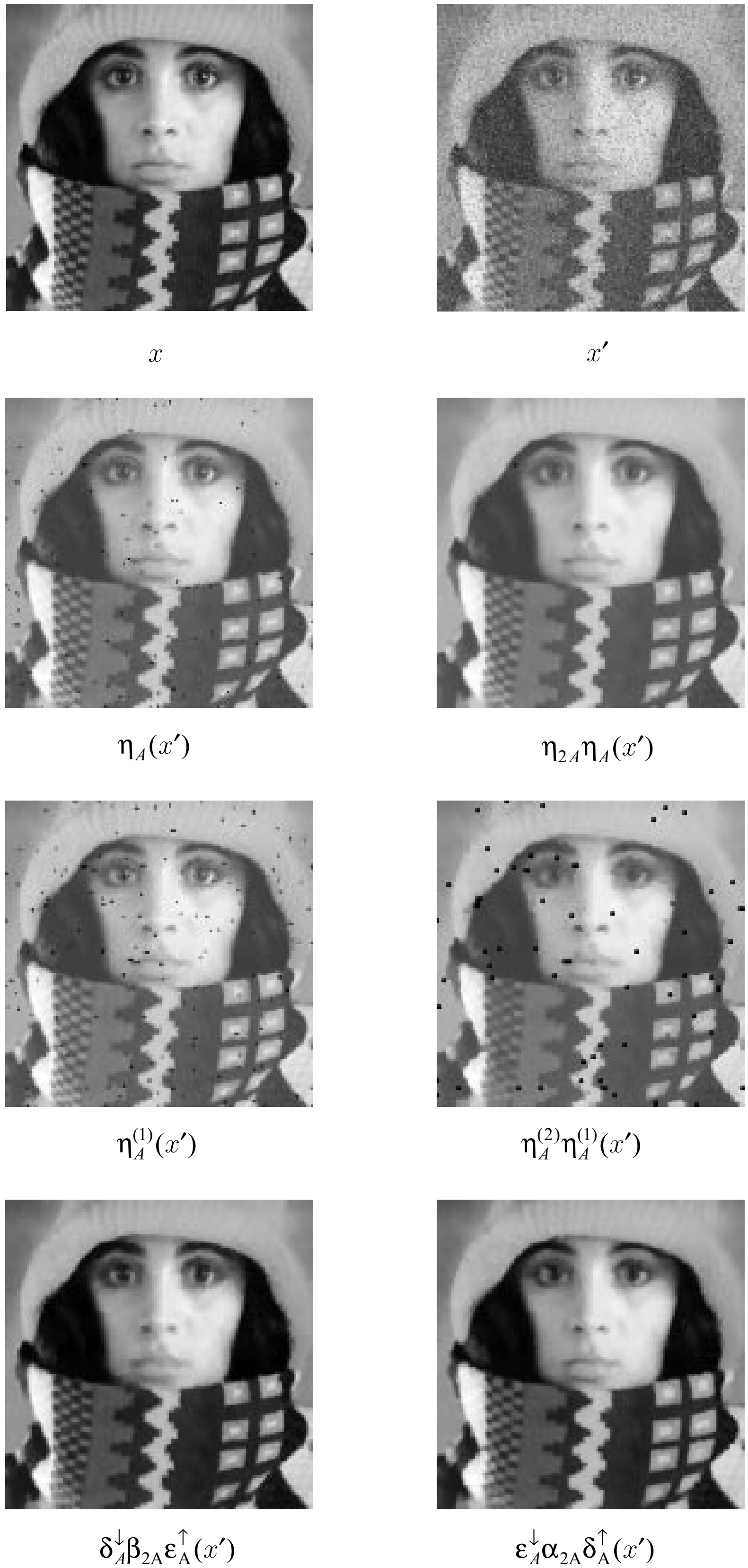

Fig. 19. A grayscale example illustrating the application of single-scale and multiscale morphological filters for noise removal. A is the 3×3 structuring element.

Consider the framework sketched at the beginning of Section 5, and define

$$\alpha_j := \hat{\psi}_{0,j} = \psi^{\downarrow}_{j,0}\psi^{\uparrow}_{0,j}, \quad \text{for } j > 0,$$

where $\psi^{\uparrow}_{i,j}$, $\psi^{\downarrow}_{j,i}$ are given by (3.1) and (3.2), respectively, with $(\psi^{\uparrow}_j, \psi^{\downarrow}_j)$ being an adjunction between the complete lattices V_j and V_{j+1}. Equation (3.5) says that

$$\alpha_j\alpha_i = \alpha_i\alpha_j = \alpha_j, \quad \text{if } j \geq i. \tag{7.4}$$

From the fact that $(\psi^{\uparrow}_{0,j}, \psi^{\downarrow}_{j,0})$ defines an adjunction between V_0 and V_j, we conclude that α_j is an opening on V_0, which, together with (7.4), results in $\alpha_{j+1} \leq \alpha_j$, for $j \geq 0$, where we set $\alpha_0 = \mathsf{id}$. Thus, we may conclude that $\{\alpha_j \mid j \geq 0\}$ defines a (discrete) granulometry. For obvious reasons, we call this family a *multiscale granulometry*, provided that $(\psi^{\uparrow}_j, \psi^{\downarrow}_j)$ is a multiscale adjunction.

In a similar fashion, we may define $\beta_j := \hat{\psi}_{0,j} = \psi^{\downarrow}_{j,0}\psi^{\uparrow}_{0,j}$, for $j > 1$, with $\psi^{\uparrow}_{i,j}$, $\psi^{\downarrow}_{j,i}$ given by (3.1) and (3.2), respectively, with $(\psi^{\downarrow}_j, \psi^{\uparrow}_j)$ being an adjunction between the complete lattices V_j and V_{j+1}. Then, the family $\{\beta_j \mid j \geq 1\}$ defines a *multiscale anti-granulometry.*

The decomposition of a signal x into the set $\{..., \beta_2(x) - \beta_1(x), \beta_1(x) - x, x - \alpha_1(x), \alpha_1(x) - \alpha_2(x), ...\}$ will be called the *multiscale discrete size transform* of x, whereas $\{..., |\beta_2(x) - \beta_1(x)|, |\beta_1(x) - x|, |x - \alpha_1(x)|, |\alpha_1(x) - \alpha_2(x)|, ...\}$, with $|x| = \sum_n |x(n)|$, will be called the *multiscale pattern spectrum* of x.

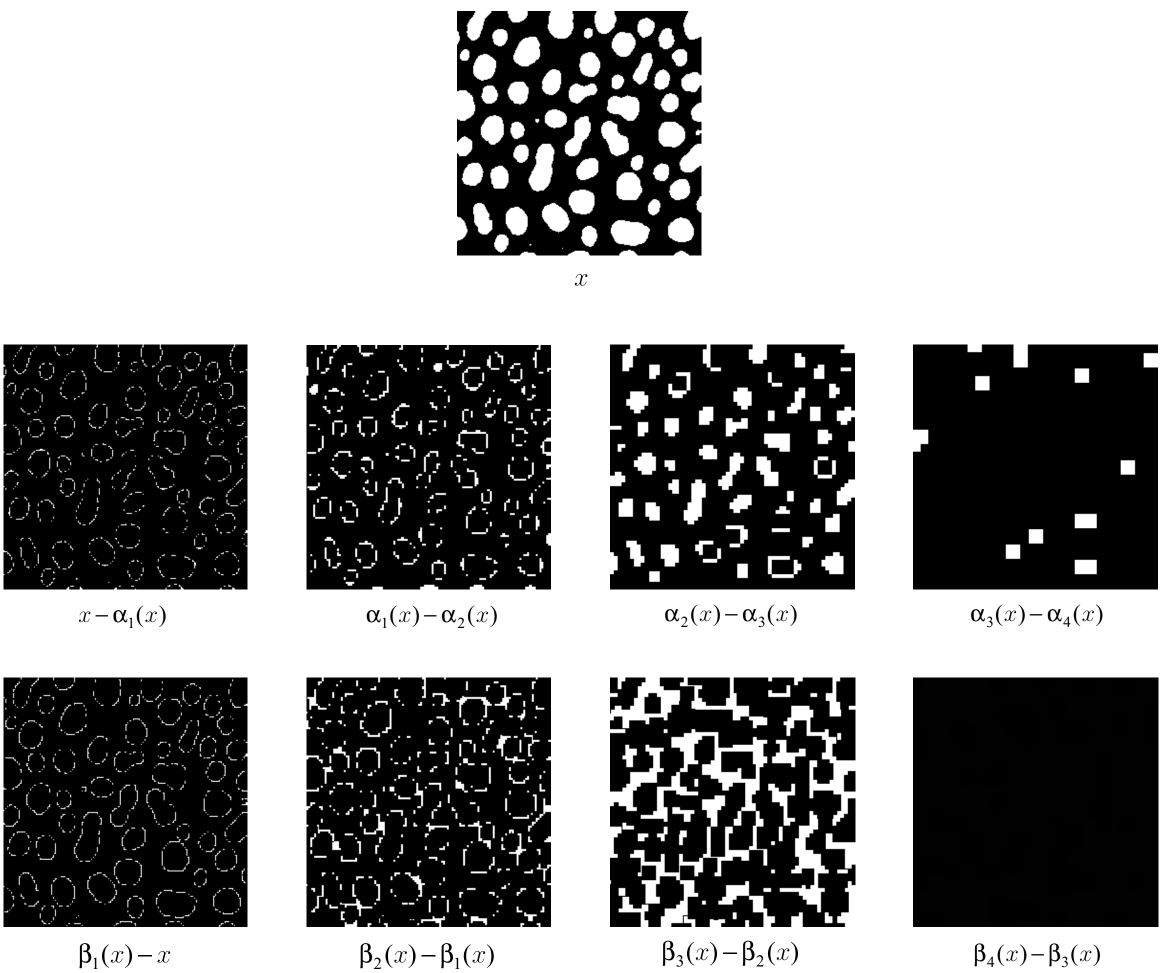

Fig. 20. The first 4 components of the multiscale discrete size transform of a binary image.

The most useful granulometry is obtained by means of the multiscale adjunction $(\epsilon_A^{\uparrow}, \delta_A^{\downarrow})$, in which case, $\alpha_j = \alpha_A^{(j)}$ and $\beta_j = \beta_A^{(j)}$, where $\alpha_A^{(j)}$ and $\beta_A^{(j)}$ are given by (7.3). Figure 20 depicts the first 4 components of the multiscale discrete size transform of a binary image, whereas Figure 21 depicts the corresponding pattern spectrum.

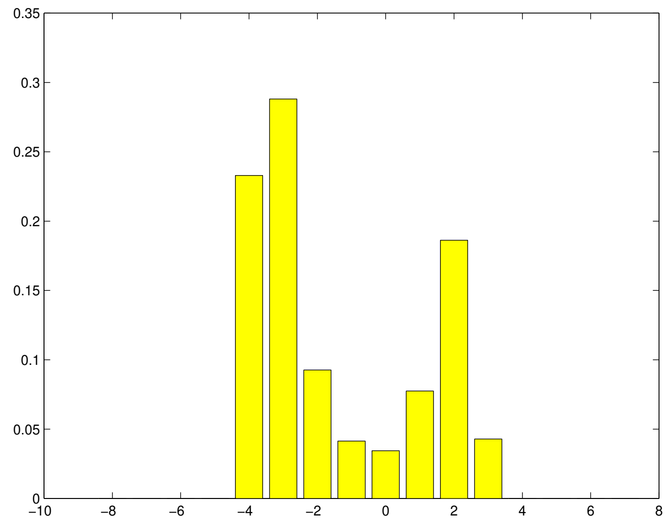

Fig. 21. The multiscale pattern spectrum associated with the binary image of Figure 20.

8. Conclusions

In this first part of our study on general linear and nonlinear multiresolution signal decomposition schemes, we have presented an axiomatic treatise of *pyramid* decomposition schemes. The basic ingredient of such schemes is the so-called *pyramid condition* which states that synthesis of a signal followed by analysis returns the original signal. This simple and intuitive condition, which means that synthesis never gives rise to (additional) loss of information, lies at the heart of various linear and nonlinear decomposition schemes. For example, the well-known Burt-Adelson pyramid fits well inside our framework, presumed that the parameters are chosen appropriately. In our exposition, we distinguish not only between linear and nonlinear (e.g., morphological) schemes, but also between *single-scale* and *multiscale* decomposition schemes; i.e., without and with sample reduction, respectively.

A great deal of attention has been devoted to morphological pyramids, in particular to pyramids where the analysis and synthesis operators constitute adjunctions between consecutive levels of the pyramid. This also leads, in a natural way, to a new family of morphological operators, the so-called *multiscale morphological operators*. Of special interest here are *multiscale granulometries*; we have found that every morphological adjunction pyramid defines a multiscale granulometry. Furthermore, a simple and straightforward application of the single-scale adjunction pyramid leads to a (minor but elegant) improvement of Lantuéjoul's skeleton decomposition.

In a second forthcoming part of our study, we shall consider wavelet decomposition schemes, comprising two (or more) analysis and synthesis operators at each level. In that study, we shall give particular attention to a new family of wavelets, the so-called *morphological wavelets*. The interested reader may refer to our conference papers [10, 9] for some preliminary results.

References

[1] Burt, P. J., and Adelson, E. H. The Laplacian pyramid as a compact image code. *IEEE Transactions on Communications 31* (1983), 532–540.

[2] Chen, R.-J., and Chieu, B.-C. Three-dimensional morphological pyramid and its application to color image sequence coding. *Signal Processing 44*, 2 (1995), 163–180.

[3] Daubechies, I. *Ten Lectures on Wavelets.* Society for Industrial and Applied Mathematics, Philadelphia, PA, 1992.

[4] Delfiner, P. A generalization of the concept of size. *Journal of Microscopy 95* (1971), 203–216.

[5] Gonzalez, R. C., and Woods, R. E. *Digital Image Processing.* Addison-Wesley, Reading, MA, 1992.

[6] Goutsias, J., and Schonfeld, D. Morphological representation of discrete and binary images. *IEEE Transactions on Signal Processing 39* (1991), 1369–1379.

[7] Heijmans, H. J. A. M. *Morphological Image Operators.* Academic Press, Boston, 1994.

[8] Heijmans, H. J. A. M. Composing morphological filters. *IEEE Transactions on Image Processing 6*, 5 (1997), 713–723.

[9] Heijmans, H. J. A. M., and Goutsias, J. Morphology-based perfect reconstruction filter banks. In *IEEE International Symposium on Time-Frequency and Time-Scale Analysis* (Pittsburgh, 1998).

[10] Heijmans, H. J. A. M., and Goutsias, J. Some thoughts on morphological pyramids and wavelets. In *Signal Processing IX: Theories and Applications (volume I)* (Rhodes, Greece, 1998), Eusipco 1998, pp. 133–136.

[11] Heijmans, H. J. A. M., and Ronse, C. The algebraic basis of mathematical morphology – part I: Dilations and erosions. *Computer Vision, Graphics and Image Processing 50* (1990), 245–295.

[12] Heijmans, H. J. A. M., and Toet, A. Morphological sampling. *Computer Vision, Graphics and Image Processing: Image Understanding 54* (1991), 384–400.

[13] Kong, X., and Goutsias, J. A study of pyramidal techniques for image representation and compression. *Journal of Visual Communication and Image Representation 5* (1994), 190–203.

[14] Kresch, R. *Morphological image representation for coding applications.* PhD thesis, Technion Israel Institute of Technology, Haifa, 1995.

[15] Kresch, R., and Malah, D. Morphological reduction of skeleton redundancy. *Signal Processing 38* (1994), 143–151.

[16] Mallat, S. *A Wavelet Tour of Signal Processing.* Academic Press, San Diego, 1998.

[17] Mallat, S. G. A theory for multiresolution signal decomposition: The wavelet representation. *IEEE Transactions on Pattern Analysis and Machine Intelligence 11* (1989), 674–693.

[18] Maragos, P. Morphological skeleton representation and coding of binary images. *IEEE Transactions on Acoustics, Speech and Signal Processing 34* (1986), 1228–1244.

[19] Maragos, P. Pattern spectrum and multiscale shape representation. *IEEE Transactions on Pattern Analysis and Machine Intelligence 11* (1989), 701–716.

[20] Matheron, G. *Random Sets and Integral Geometry.* John Wiley & Sons, New York, 1975.

[21] Matsopoulos, G. K., and Marshall, S. Application of morphological pyramids: fusion of MR and CT phantoms. *Journal of Visual Communication and Image Representation 6*, 2 (1995), 196–207.

[22] Mattioli, J., and Schmitt, M. Inverse problems for granulometries by erosion. *Journal of Mathematical Imaging and Vision 2* (1992), 217–232.

[23] Montiel, M. E., Aguado, A. S., Garza-Jinich, M. A., and Alarcon, J. Image manipulation using M-filters in a pyramidal computer model. *IEEE Transactions on Pattern Analysis and Machine Intelligence 17*, 11 (1995), 1110–1115.

[24] Morales, A., Acharya, R., and Ko, S.-J. Morphological pyramids with alternating sequential filters. *IEEE Transactions on Image Processing 4*, 7 (1995), 965–977.

[25] Overturf, L. A., Comer, M. L., and Delp, E. J. Color image coding using morphological pyramid decomposition. *IEEE Transactions on Image Processing 4*, 2 (1995), 177–185.

[26] Rioul, O. A discrete-time multiresolution theory. *IEEE Transactions on Signal Processing 41* (1993), 2591–2606.

[27] Serra, J. *Image Analysis and Mathematical Morphology.* Academic Press, London, 1982.

[28] Serra, J., and Vincent, L. An overview of morphological filtering. *IEEE Transactions on Circuits, Systems and Signal Processing 11* (1992), 47–108.

[29] Song, X., and Neuvo, Y. Image compression using nonlinear pyramid vector quantization. *Multidimensional Systems and Signal Processing 5* (1994), 133–149.

[30] Strang, G., and Nguyen, T. *Wavelets and Filter Banks.* Wellesley-Cambridge Press, Wellesley, MA, 1996.

[31] Sun, F.-K., and Maragos, P. Experiments on image compression using morphological pyramids. In *Visual Communications and Image Processing '92* (Philadelhia, Pennsylvania, 1989), vol. 1199 of *SPIE Proceedings.*

[32] Toet, A. A morphological pyramidal image decomposition. *Pattern Recognition Letters 9* (1989), 255–261.

[33] Vetterli, M., and Kovacevic, J. *Wavelets and Subband Coding.* Prentice Hall, Englewood Cliffs, NJ, 1995.